TECHNISCHE UNIVERSITÄT MÜNCHEN

Klinik für Plastische und Handchirurgie

The Use of Cell-based Approaches for Inducing Therapeutic Vascularization

Ziyang Zhang

Vollständiger Abdruck der von der Fakultät für Medizin der Technischen Universität München zur Erlangung des akademischen Grades eines

Doctor of Philosophy (Ph.D.)

genehmigten Dissertation.

Vorsitzender: Univ.-Prof. Dr. Bernd Gänsbacher

Prüfer der Dissertation:

1. Univ.-Prof. Dr. Hans-Günther Machens

2. Univ.-Prof. Dr. Steffen Massberg

Die Dissertation wurde am 13.01.2012 bei der Fakultät für Medizin der Technischen Universität München eingereicht und durch die Fakultät für Medizin am 21.02.2012 angenommen.

ABSTRACT

Background: The aim of the present PhD thesis is to evaluate the possible utilization of different cell-based therapies for treating ischemia-related clinical problems, especially chronic wounds. Vascularization is a key process in tissue engineering and regeneration. It represents one of the most important issues in the field of regenerative medicine. Cell-based therapies are of great interest to researchers due to the improvement of stem/progenitor cell technology and also the improvement of the genetic modification technology of cells. Several cell-based strategies aimed to improve vascularization are currently under pre-clinical or clinical evaluation.

Materials and methods: We evaluated three different cell-based therapies using two different ischemic tissue regeneration models: 1) Stem cells derived from human sweat glands were isolated, characterized and seeded in collagen scaffold, and engrafted in a mouse full skin defect model for evaluating dermal neovascularization. 2) We isolated and characterized vascular resident endothelial progenitor cells (VR-EPCs) from cardiac tissue *in vitro*, evaluating their regenerative potential *in vivo* in a bare mouse full skin defect model to test the neovascularization ability of such cells. 3) During the first two sub-projects, we discovered the paracrine effects from stem/progenitor cells secreting pro-angiogenic factors. Thus, rat dermal fibroblasts were nucleofected *ex vivo* to release pro-angiogenic factors bFGF and VEGF165 and applied in a hind limb ischemia model *in vivo to* test the contribution of paracrine effects for neovascularization. After femoral artery ligation, gene-modified cells were injected intramuscularly. One week post injection, local confined plasmid

expression and transient distributions of the plasmids in other organs were detected by quantitative PCR. Quantitative micro-CT analyses showed improvements of vascularization in the ischemic zone.

Principle findings: 1) The presence of human sweat gland-derived stem cells significantly improved dermal neovascularization ($p<0.001$). 2) The presence of VR-EPCs enhanced dermal vascularization area ($p<0.001$). Histological assays showed increased vessel number ($p < 0.05$) and cellularization ($p < 0.05$). 3) Quantitative micro-CT analyses showed improvements of vascularization in the ischemic zone in the hind limb ischemia model. Moreover, improved collateral proliferation and an increase in blood perfusion in the lower hindlimb were also observed.

Conclusions: These results demonstrate the feasibility and effectiveness of cell-based therapies in different ischemia-related problems. Possible candidate cells discussed in this thesis include: 1) sweat gland-derived stem cells; 2) highly clonogenic therapeutic population of VR-EPCs; 3) gene nucleofected primary fibroblasts producing pro-angiogenic growth factors.

ACKNOWLEDGEMENTS

This thesis is considered my last piece of work during my student period. It marks the end of my approximately 12 years of medical and biological studies. In other words, I will not get any discounts as a student anymore, and I need to pay tax now.

First and foremost I would like to thank my supervisor Prof. Dr. med. Hans-Günther Machens for his constant support during the past years. I would like to thank him for a lot of things, but one most important thing for me is that whenever I needed his help, he was always there.

Many thanks to all the people who helped me with this PhD work. I am very grateful for the support I got from everyone of you. Without your tolerance of my periodic laziness and mistakes, I would not have survived this physically and mentally intensive and challenging PhD program.

Special thanks to:

Prof. Dr. med. Arndt F. Schilling, Prof. Jihong Liu, Dr. Wulf D.Ito, Dr. Tomás Egaña, Dr. Slobodianski, Mrs. Astrid Arnold, Mrs. Ursula Hopfner, Mr. Mark di Frangia.

Last but not the least I would like to thank my family members:

I thank my wife for taking care of me all the time!

I thank my parents for supporting me for all these years!

PUBLICATIONS RELATED TO THIS THESIS

1) Zhang Z, Ito WD, Hopfner U, Böhmert B, Harder Y, Reckhenrich AK, Kremer M, Lund N, Kruse C, Machens HG Egaña JT *. The Role of Single Cell Derived Vascular Resident Endothelial Progenitor Cells in the Enhancement of Vascularization in Scaffold-based Skin Regeneration. *Biomaterials*. 2011 Jun; 32(17):4109-17. Epub 2011 Mar 23. (Impact factor 2010: 7.8)

2) Zhang Z, Slobodianski A, Ito W.D, Kathöfer A, Frenz, Weng S, Lund N, Liu J, Egana JT, Lohmeyer JA , Müller DF. Machens HG. Enhanced Collateral Growth by Double Transplantation of Gene-Nucleofected Fibroblasts in Ischemic Hindlimb of Rats. *PLoS ONE* 6(4): e19192. doi:10.1371/journal.pone.0019192 (Impact factor 2010: 4.4)

3) Zhang Z, Slobodianski A, Arnold A, Nelsen J, Hartog C, Hopfner U, Reckhenrich AK, Egaña JT, Schilling AF, Liu J, Lohmeyer JA, Machens HG. Improved Nucleofection Method for Transfection of Dermal Fibroblasts- A Translational Therapeutic Approach for Cell-based Gene Therapy (In preparation)

4) Danner S, Kremer M2, Petschnik AE, Nagel S, **Zhang Z**, Hopfner U, Reckhenrich AK, Weber C, Schenck TL, Becker T, Kruse C, Machens HG, Egaña JT. The Use of Human Sweat Gland-derived Stem Cells for Enhancing Vascularization during Dermal Regeneration. (Accepted by *Journal of Investigative Dermatology* Impact factor 2010: 6.2)

FUNDING RELATED TO THIS THESIS

1) Clinical research grant from Technische Universität München to Dr.med. Ziyang Zhang (KKF. No. 8744556)

2) Innovations Fund of Schleswig-Holstein to Prof. Hans-Günther Machens

3) A scholarship from the China Scholarship Council to Dr.med. Ziyang Zhang

4) German Research Foundation (DFG) IT-13/1, IT- 13/2 and IT-13/3 to Dr. Wulf D. Ito

5) European Fund for Regional Development (EFRE) to Prof. Charli Kruse

TABLE OF CONTENT

LIST OF FIGURES AND TABLES

LIST OF ABBREVIATIONS

BrdU	5-bromo-2deoxyuridine
BSA	Bovine Serum Albumin
CD	Cluster of Differentiation
CT	Computer Tomography
DMEM	Dulbecco's Modified Eagle's Medium
DNA	Deoxyribonucleic acid
EDTA	ethylenediaminetetraacetic acid
EPCs	Endothelial Progenitor Cells
FACS	Fluorescence Activated Cell Sorting
FCS	Fetal Calf Serum
FLk	Fetal liver kinase
FLt	Fms-related tyrosine kinase
GFP	Green fluorescence protein
IgG	Immunoglobulin G
PBS	Phosphate Buffer Saline
VR-EPCs	Vascular resident endothelial progenitor cells
vWF	Von Willebrand factor
3-D	Three dimension
VEGF	Vascular endothelial growth factor
bFGF	Basic fibroblast growth factor
PDGF	Platelet-derived growth factor
HLA	Human leukocyte antigen
MSCs	Mesenchymal stem cells
EPCs	Endothelial progenitor cells
VR-EPCs	Vascular resident endothelial progenitor cells
ECM	Extra cellular matrix
ACT	Autologous cell therapy
hESCs	Human embryonic stem cells
ECFCs	Endothelial colony forming cells
EPO	Erythropoietin

1. INTRODUCTION

1.1 Chronic wounds of the lower extremity

A chronic wound of the lower extremities is a well-known problem in plastic surgery department with a high prevalence in the elderly (Figure1). It affects over 6 million people in the U.S. The prevalence of chronic limb ulceration is around 15 percent and is expected to reach 25 percent by the year 2050 [1].

The mostly affected organ during chronic wounds is the skin. Although not obvious, skin is actually the largest organ of the human body. It acts as the first defense barrier when the human body comes into contact with the environment. As shown in Figure 2, skin can be divided into three basic layers: epidermis, dermis and hypodermis. It contains several inner components, such as sweat glands, blood vessels, collagen, hair follicles, fibroblasts and keratinocytes. Under normal conditions, the skin, like other organs of the human body, can heal itself by production and degradation of several important molecules and reform blood vessels, fibroblasts and collagen. However, chronic wounds seem to be trapped in a certain stage of healing process and thus cannot balance the production and degradation of these molecules [2].

Besides skin, another usually affected structure is actually vessels from the lower extremities. Many diseases can cause the ischemia of the lower limbs (Figure 3). Peripheral artery disease, which is characterized by the narrowing of limb artery and reduced blood flow, is one of the major causes for leg/foot chronic wounds [3]. Insufficient blood supply always causes chronic wounds or even gangrene in the ischemia area.

Figure 1: Chronic wound in the lower extremities. Typical chronic wounds prior to debridement (modified from Paul J. Kim et al. 2007)

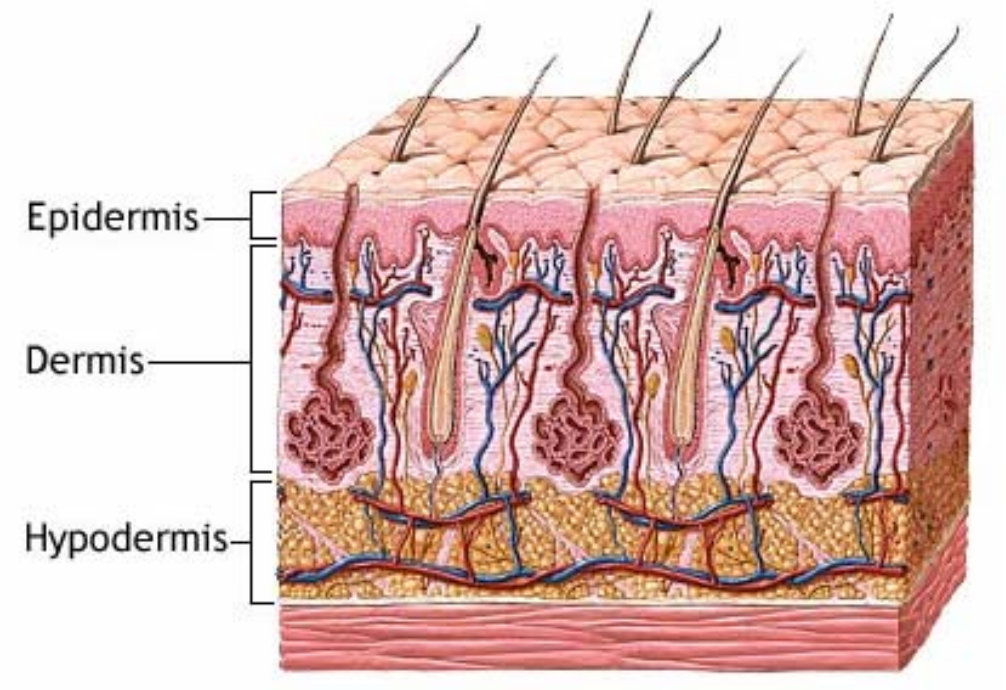

Figure 2: Structure of the skin. Skin can be divided into three layers: epidermis, dermis and hypodermis. Sweat glands are inside the dermis layer. (Modified from http://www.nlm.nih.gov)

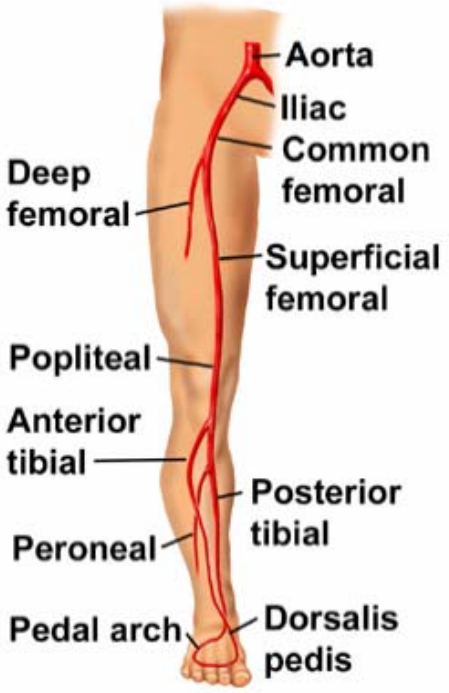

Figure 3: Major blood supply vessels in human lower limbs. (Modified from http://www.carolinavascular.com)

Normal wound healing is a complex physiological process which involves many different steps. Under physiological conditions, a wound usually heals within a certain amount of time. It is one of the most important functions of our human body. However, under pathophysiological conditions, or when a large wound defect occurs, wound healing often becomes very difficult. Thus, the wounds will often become chronic.

Under physiological conditions, a wound will cause a healing response and an intact healing process can be expected. Wound healing after skin tissue injury is a complex process which involves several steps such as: blood clotting, platelet aggregation and leukocytes migration [4]. The clotting of fibroin in the blood, which is an initial step of wound healing, can provide a local scaffold for cell migration and growth. Migrated cells (macrophages and neutrophils) and

local cells (surrounding fibroblasts and endothelial cells) can then interact with each other and secret growth factors to induce microvasculature formation. Granulation tissue, which is mainly formed by fibroblasts, extracellular matrix (ECM) and newly formed vessels, will start to form around day 5 and replace the fibrin clot. The granulation tissue can normally cover the whole wound area and the new tissue will be formed from local cells, migrated cells and ECM. In all the above steps, local blood vessel formation is the most important step, since the newly-formed tissue will need blood vessels to bring the nutrients and immune cells to kill the microorganisms and moreover, to take away the wastes. Under pathophysiological conditions (e.g. bacteria infection) the wound healing process is always blocked mid-way. The bacteria can produce polysaccharides to protect themselves from the phagocytes in the local wound environment. The phagocytes, will release several toxic agents including oxygen radials to exterminate the bacteria. The result of this battle is the impairing of the local environment and thus a delayed or even halted wound healing process.

There are several kinds of clinical treatments available currently for non-healing chronic leg/foot wounds. The first step of all these treatments is called debridement, which means getting rid of dead tissue and then a thorough disinfection. After this, depending on the doctor or hospital, there are several different choices. Very often, a dressing is then applied to the wounded area. A dressing is designed to keep the wound area moist and protect the wound from infectious sources. It directly contacts the wound surface and promotes wound healing. There are dozens of commercially available

dressings for the purpose of wound healing as listed online (http://www.dressings.org). Besides dressing, other technical devices can also be used for wound healing. However, they are not generally accepted as standard procedures. These treatments including 1) Laser therapy [5]; 2) Oxygen chamber [6]; 3) Vacuum assistant wound closure [7]; 4) non-thermal argon plasma [8].

When a large skin defect occurs (e.g., burn injury, trauma, or chronic wounds), the gold standard is still the use of split-thickness skin grafts. A split-thickness skin graft is a skin graft containing the epidermis and part of the dermis. It is used in clinics for covering large or full thickness skin defects. However, besides the possible donor side morbidity and the shortage of healthy skin grafts, the split-thickness skin grafts can merely restore part of the full skin function, and this can lead to a contraction of the grafts and therefore scar formation. As a result, a tissue-engineered artificial skin scaffold is an alternative approach in the future (Figure 4).

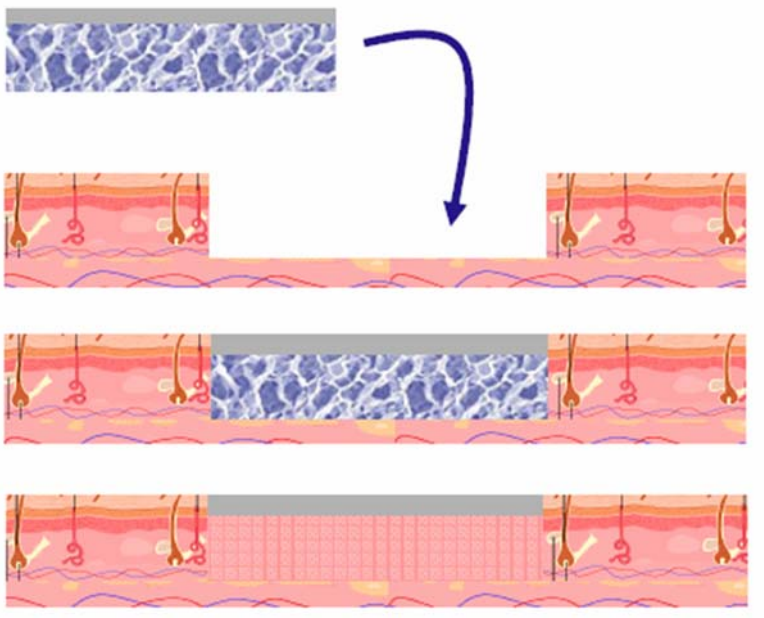

Figure 4: Scheme of artificial skin scaffold application. Two-layer skin scaffold is

sutured for covering the wound and then degraded *in vivo* by the newly formed tissue.

1.2 Cell-based therapy

Cell based therapies are defined as the use of certain cells with therapeutic potential for treating diseases. Based on the cells used in such therapies, they can be divided into two categories: autologous cell-based therapy and heterologous cell-based therapy

Autologous cell-based therapy (ACT) is a clinical intervention based on the cells from individual patients. Cells will be first isolated from the tissues of the individuals and then expanded and even modified *in vitro*. After that, cells will be reapplied to the same donor. The major advantage of such approach is the minimization of immunological reactions and no possible disease transfer from other donors. The cell source in this situation is not limited to a certain kind of cell population but all kinds of cells that are useful to the donor patient. For example, for skin wounds, it is possible to use fibroblasts combining with an artificial skin scaffold to enhance the wound healing [9]. As shown in figure 5, autologous mesenchymal stem cells (MSC) delivered in a fibrin spray can also accelerate the wound healing in a chronic wound patient [10]. Most important, with improving gene modification technology, it is possible to modify the autologous cells to express therapeutic genes. Autologous dermal fibroblasts from rabbits were tested with a virus-based pro-angiogenic gene transfer method in a hind limb ischemia model. After the injection of VEGF and bFGF expressing fibroblasts, enhancement of neovascularization effects was observed and it is better than using a single pro-angiogenic factor [9]. However,

one major disadvantage of autologous cell therapy is the limited amount of cells from an individual patient. The clinical conditions of patients are usually not good enough to isolate large amounts of cells for *in vitro* expanding. In this situation, heterologous cell-based therapy is needed.

Although most of the cell therapies are based on autologous cells, heterologous cell-based therapy is still very often needed in the clinics. For example, when patients have multiple myeloma or leukemia, it is not possible to isolate haematopoietic stem cells autologously. Despite this, one major drawback of using heterologous cell-based therapy is the possible immune reaction related to the transplanted cells. In this case, a HLA (Human leukocyte antigen) matched allogeneic cell transplant is needed. Despite the fact that we are doing more and more HLA-matched transplantation in the world, it is still not enough considering the large amount of patients. Thus, human embryonic stem cells (hESCs), which can be differentiated into nearly all kinds of cells and have a very low immune resistance after *in vivo* delivery, have showed a huge potential for therapeutic purposes. Cardiac cells can be induced from embryonic stem cells and thus used for clinical purposes [11]. Although hESCs are very promising in a lot of pre-clinical studies, it is difficult to transfer them to the clinical level due to ethical reasons [12]. The discovery of induced pluripotent stem cells (iPSCs) provides researchers with a new hope for using stem cell therapy [13]. With a few gene modification processes, skin fibroblasts can be induced to pluripotent stem cells. Moreover, the discoveries of adult stem/progenitor cells that can contribute to neovascularization make it necessary to test them at pre-clinical levels [14, 15].

Figure 5: Use of Mesenchymal stem cells for human chronic wounds. The non-healing wound over the ankle of the patient (A) is applied with fibrin spray containing MSCs (B). After 3 months, the wound starts to fill with new tissue (C) and after 6 months the wound has healed completely (D). (Modified from Falanga et al. 2007)

1.3 Vasculature regeneration

Vasculature regeneration refers to the processes that form new types of vessels. There are three different kinds of regeneration processes, vasculogenesis, angiogenesis and arteriogenesis.

Vasculogenesis refers to the formation of new blood vessels by new endothelial cells production without pre-existing blood vessels (Figure 6A). Unlike other typical neovascularization processes, it requires mainly the stem/progenitor cells to form the new vessel structures. Vasculogenesis was originally considered to happen only during the embryonic development stage

but not in the adult stage during human development. However, the discovery of adult endothelial progenitor cells (EPCs) in 1997 showed the possibility of adult vasculogenesis [16]. EPCs can differentiate into endothelial cells *in vitro* and in animal models of ischemia; EPCs were shown to incorporate neovascularization [17] into the sites. However, although EPCs can contribute to vessel formation, they cannot form other components such as the smooth muscle cells also needed for vessel formation. So far, there are also not any stem/progenitor cells that can only form both endothelial cells and smooth muscle cells. Thus, use of stem cells, which possess multipotent differentiation ability for vasculogenesis, is also another possible method for neovascularization.

Angiogenesis is defined as the sprouting of new blood vessels from the nearby pre-existing blood vessels (Figure 6B). Although angiogenesis is not the only mechanism of vessel formation in the human body, it is the most popular one among neovascularization researchers due to the importance of angiogenesis for many physiological and/or physiopathological processes. There are now more than 50,000 scientific publications about angiogenesis. A British surgeon, Dr. John Hunter, first used it to describe blood vessels growing in the reindeer antler. Angiogenesis is usually triggered in physiological conditions by the local release of hypoxia-inducible factor-1 (HIF-1α) [18]. HIF-1α can then drive the local release of several important pre-angiogenic factors, such as vascular endothelial growth factor (VEGF), basic fibroblasts growth factor (bFGF), platelet-derived growth factor (PDGF) and erythropoietin (EPO). Under pathophysiological conditions any diseases that cause hypoxia will trigger the

release of HIF-1α and can induce angiogenesis. In children, angiogenesis happens after the building of major blood vessels by vasculogenesis. Thereafter, angiogenesis helps the body to enhance the vessel network by extending the blood vessels from existing major stem vessels. In adults, besides the blood vessel formation during the menstrual cycle in women, angiogenesis plays a major role during the wound healing process.

Arteriogenesis was invented in 1996 by a group of scientists in Europe; it was then widely spread into the neovascularization research field [19]. Arteriogenesis is the process when a preexisting arteriole is adapted into a mature conductance artery under the shear stress caused by an artery occlusion (Figure 6C and Figure 7). It is actually the morphological change of the preexisting arterioles. The main function of arteriogenesis during the physiological or pathophysiological processes is to maintain the tissue blood perfusion. It can compensate for an occluded artery. Some researchers believe that arteriogenesis and angiogenesis are two separate processes, which are triggered by different cellular and molecular mechanisms. For example, in a hind limb ischemia model, it is believed that arteriogenesis is the dominant physiological process which happens only in the upper leg close to the occlusion point whereas angiogenesis contrarily happens only in the lower leg and foot part [20]. However, some researchers believe that the two processes can be triggered by the same factors [21].

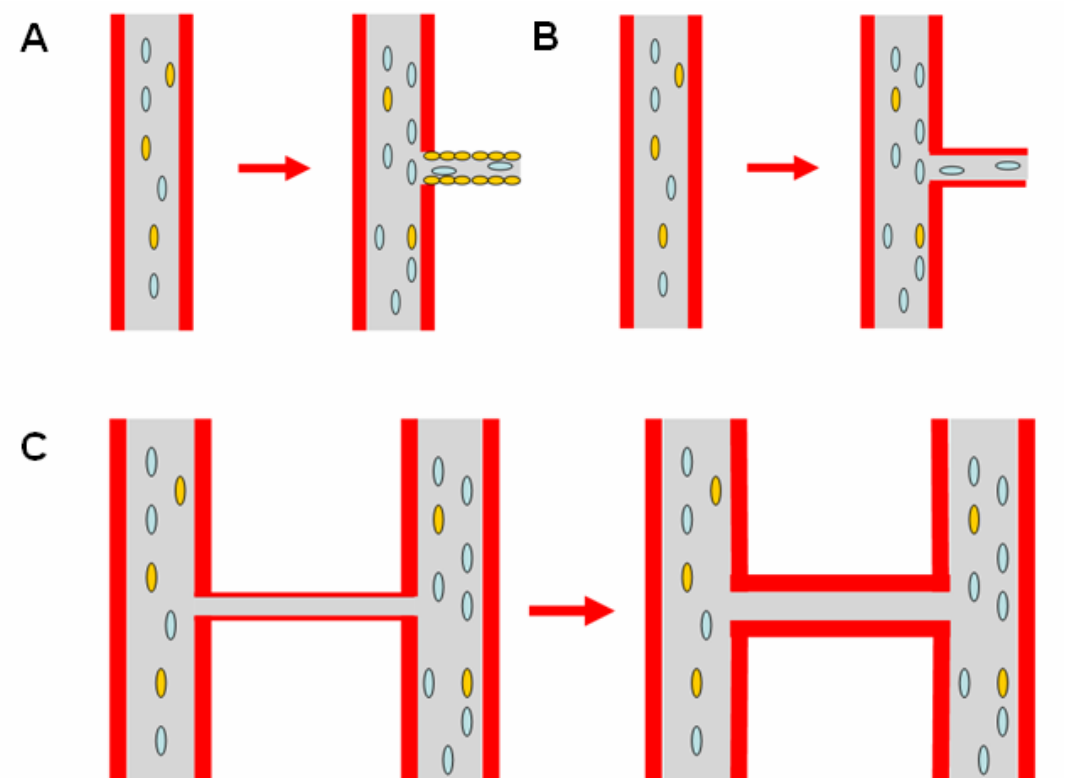

Figure 6: Three mechanisms for neovascularization: vasculogenesis, angiogenesis and arteriogenesis. (A) Vasculogenesis is the *de novo* formation of blood vessels from blood vessel forming angioblasts (yellow dots). (B) Angiogenesis is the formation of blood vessels from pre-existing nearby vessels (C) Arteriogenesis is responsible for the growth of collateral arteries from pre-existing arteriolar anastomoses in conditions of ischemia; it helps the tissue to regain the blood perfusion by changing the morphology of small vessels.

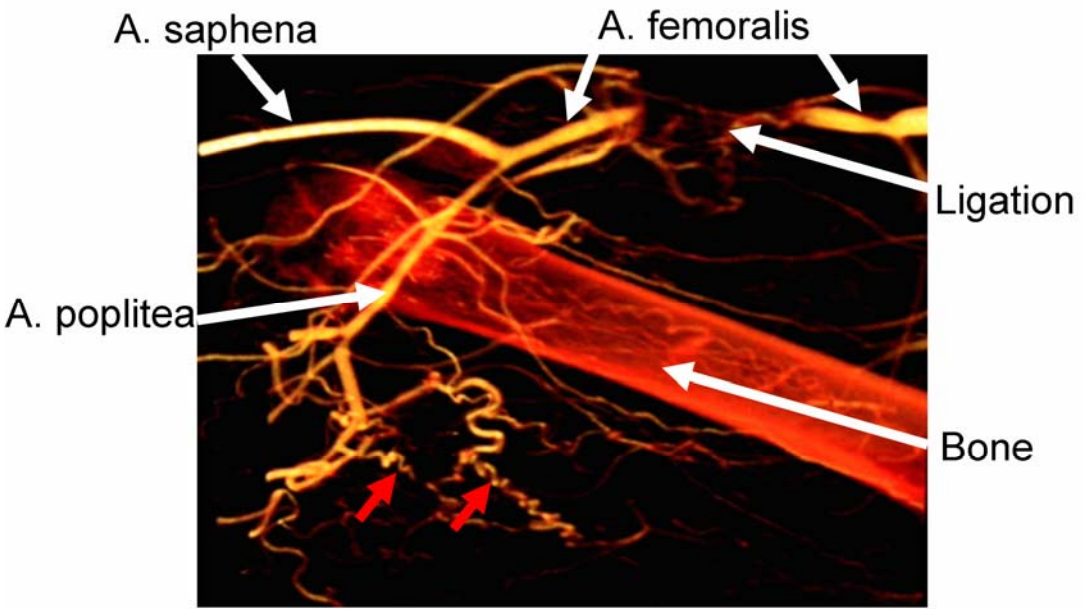

Figure 7: Anatomical view of micro-CT reconstruction from a rat hind limb ischemia model. The figure shows a clear ligation of the femoral artery from the upper part of the hind limb. The red arrows indicate the collateral vessels which are the major blood vessels perfusing the lower limb after femoral artery occlusion.

1.4 Stem cells and therapeutic vascularization

Stem cells are defined by their multipotent differentiation ability and a high potential for self-renewal. Basically, stem cells can be isolated from both embryonic and adult tissues. Embryonic stem cells are mostly involved in the body development and can be only isolated in embryonic tissues. On the contrary, adult stem cells can be found in different adult tissues and organs, such as: adipose tissue[22], bone marrow[23], glands[24], skin[25], blood[26], vessel wall[14]. Embryonic stem cells are considered as totipoent cells since they are differentiated into embryonic tissue and extraembryonic tissues. Adult stem cells are nearly all multipotent cells; they can only differentiate into some closely related family cells. Although it seems embryonic stem cells are more

promising compared to adult stem cells for clinical purposes, embryonic stem cells are not popular for researchers due to ethical reasons and possible uncontrolled *in vivo* differentiation.

Under proper differentiation conditions, adult stem cells can be differentiated into the cells that can help body repair. Adult stem cell differentiation is related to the stem cell microenvironment, in other words, to stem cell niches. When we implant stem cells into tissues or organs, it is important to notice the potential differentiation changes with different stem cell niches even when we use exactly the same stem cells. For instance, human adipose tissue-derived stem cells can promote angiogenesis and differentiate into myocytes [27]. Neural stem cells were found to produce muscle when they were implanted into skeletal tissues [28]. Thus, the transplantation of adult stem cells into the ischemic tissue or organ for therapeutic neovascularization is a prominent tool for clinicians. Several studies have proved the use of adult stem cells for enhancing vessel formation within scaffolds for tissue regeneration. Hypoxia preconditioned mesenchymal stem cells can improve vascular and muscular regeneration in a hind limb ischemia model [29]. Human mesenchymal stem cells were used to improve vascularization in a mouse scaffold-based skin regeneration model [30]. Although bone marrow-derived mesenchymal stem cells are still the most popular adult stem cells for tissue regeneration research, other sources are still needed. Recently, multipotent stem cells obtained from mouse pancreas and submandibular glands were tested for *in vivo* vascularization [31, 32]. Both direct differentiation and paracrine effects have contributed to the neovascularization effects. This study proves the possible

use of gland-derived stem cells for therapeutic neovascularization. However, both pancreas and submandibular glands are nearly impossible to obtain at a clinical level. Thus, new sources of such cells, especially human gland-derived stem cells, are still needed.

1.5 Endothelial progenitor cells and therapeutic vascularization

Unlike stem cells, progenitor cells are usually unipotent, which means they can only differentiate into one specific cell type. However, some progenitor cells can actually differentiate into not just one type of cells. Thus, the definition of a progenitor cell is still controversial. In theory, these cells are believed to be at the stage between stem cells and fully differentiated cells. Until now, however, there are still no universal ways to define the so-called “middle stage”, and different progenitor cells are very different from each other. Although named differently, progenitor cells are found in many tissue or organs. Vascular progenitor cells are circulation cells that can differentiate into endothelial cells and smooth muscle cells, and they have recently been found to play a role in diagnosing polycystic ovarian syndrome [33]. In bone marrow, a CD34+/M-cadherin+ bone marrow progenitor cell is more efficient enhancing arteriogenesis than normal bone marrow stem cells in a hind limb ischemia model [34]. Neural progenitor cells can be the target cells for treating neural degeneration diseases [35].

Table 1 Comparison of stem cells and progenitor cells

	Stem cells	Progenitor cells
Cell potency	**Multipotent**	**Unipotent**
Tumorigenesis	**Yes**	**No**
Self-renewal ability	**Unlimited**	**Limited**
Source / isolation	**Embry** **Adult organ** **Gene induced**	**Stem cells** **Adult organ**

Endothelial progenitor cells (EPCs) are progenitor cells that are considered to only have the ability to differentiate into endothelial cells. However, the exact location and definition of such cells is still under controversial. The first publication about such cells is in 1997 [16]. In this paper, CD34+ Flk1+ human peripheral blood mononuclear cells were isolated and applied *in vitro* and *in vivo* in a hindlimb ischemia model. The cells could not only form capillary like structures *in vitro* and could contribute to the *in vivo* neovascularization in a nude mouse hind limb ischemia model. After the publication of this finding, CD34 + is used as a major marker for endothelial progenitor cells isolation. However, several later publications have also used CD133 as an endothelial progenitor cell marker [36]. Even CD133 alone can be used to isolate endothelial progenitor cells [37]. Since CD133 and CD34 are also expressed on the haemopoietic stem cells, a contamination of haemopoietic stem cells is expected [38]. Interestingly, two populations of EPCs were actually found in the peripheral blood cells: early EPCs and late EPCs [39]. Recently, aimed to isolate a more pure population of endothelial progenitor cells, single cell clonogenic assay was used to isolate endothelial progenitors from periphery

blood cells [40], these cells are named endothelial colony forming cells (ECFCs). One of the prestige characters of ECFCs is the nearly unlimited proliferative potential, unlike other types of endothelial progenitors; ECFCs can be cultured for a longer time without losing its neovascularization ability. Moreover, the whole population is from one single cell clone, which means these cells are highly purified cells.

EPCs can be isolated from many sources; the two major sources are peripheral blood and bone marrow. Few researches have focused on tissue resident endothelial progenitor cells. In 2001, it was proved for the first time that local endothelial progenitors are involved in the formation of human micro vessels [41]. A progenitor cell layer in the external layer of the embryonic aorta wall was found by aortic ring assay in this study. Recently, another group also found a layer in the vessel wall containing endothelial progenitors in adult human arteries [14]. Thus, in the present study, we identified a group of endothelial progenitor cells from a group of self-immortalized vasculature cell population for therapeutic neovascularization. To prove our hypothesis, we characterized them *in vitro* and *in vivo* for dermal regeneration.

1.6 Therapeutic neovascularization with growth factors

Vascular endothelial growth factor (VEGF) is one of the most studied neovascularization-related growth factors. VEGF stimulates angiogenesis [42], vasculogenesis [43] and arteriogenesis [44]. These effects are induced mainly via the stimulation of endothelial cell mitogenesis and cell migration. VEGF is produced by many different cells that stimulate the neovascularization process.

For example, VEGF can be produced by human and mouse breast fibroblasts [45] and also human lung fibroblasts [46] under different stimulations. Also some stem cells or progenitor cells can not only form vessels themselves, but also produce VEGF in a paracrine manner [31, 47]. VEGF can be classified via the different splicing of VEGF mRNA sequence. Different splicing of the exon will produce isoforms with different numbers of amino acids. For example, VEGF 165 and VEGF 121 are having 165 and 121 amino acids respectively [48]. Both VEGF 165 and VEGF 121 are both soluble VEGF isoforms and VEGF 165 is the most abundant form in human body [49]. Thus, a lot of studies have use VEGF 165 as a therapeutic factor for treating ischemia-related disease. Basic fibroblasts growth factor (bFGF) is a member of the fibroblast growth factor family. It was first discovered by Shing et al. in 1984 as a tumor-derived factor which can stimulate chick chorioallantoic membrane (CAM) vessel formation through stimulating the proliferation endothelial cells [50]. The most investigated FGF proteins are FGF2 (basic FGF). bFGF can stimulate endothelial cells mitosis and migration *in vivo*, which is the driven force of bFGF's neovascularization effects. Several early pre-clinical studies have shown that bFGF promote the wound healing process in rats by accelerating neovascularization, granulation and epithelization [51, 52]. Thus, in the last decade, several clinical trials have been conducted using bFGF as a therapeutic factor for skin wounds. Fu et al. evaluated the effect of a recombinant bovine basic fibroblast growth factor for treating burn wounds and chronic dermal ulcers [53]. Compared to the placebo group, bFGF accelerates the healing of both second-degree burns and deep second-degree burns. Nearly all the chronic wound patients healed within 6 weeks after the treatment.

In another recent clinical trial, Uchi et al. showed that a higher concentration of bFGF has a better cure rate for diabetic ulcer [54].

There are also other pro-angiogenic growth factors besides those mentioned above. Platelet-derived growth factor (PDGF) is another well-studied growth factor during neovascularization. Though it is originally found to be released by a platelet upon activation, it is believed that PDGF can also be released by several other cell types such as human bone marrow-derived stem cells [55], human embryonic stem cells [56] and endothelial progenitor cells [47]. The neovascularization effect of PDGF is related to its driven role in many cell functions such as migration, differentiation and proliferation. In addition, it is also involved in tissue remodeling and regeneration [57]. Although the main function of erythropoietin (EPO) is to control blood cell production, it is another growth factor related to neovascularization. EPO is produced mainly the peritubular capillary endothelial cells in the kidney and liver. It is also found in many other organs like the brain, bone marrow and lung at a genetic level [58]. The angiogenesis effect of EPO is believed to be related to its role in endothelial proliferation and migration since an EPO receptor is found on human endothelial cells [59]. Besides angiogenesis, EPO is also involved in the vasculogenesis by direct mobilization of bone marrow-derived endothelia progenitor cells into the circulation to form new vessels [60].

2. HYPOTHESIS

The use of stem/progenitor cells or genetically-modified cells can improve neovascularization in preclinical models of tissue ischemia and regeneration.

3. OBJECTIVES

3.1. General objective

To induce neovascularization *in vivo* using stem/progenitor cells or genetically modified cells in preclinical models of ischemia and tissue regeneration

3.2. Specific objectives

3.2.1. To study the potential use of human sweat gland-derived stem cells to induce therapeutic vascularization in scaffold-based dermal tissue engineering

3.2.2. To determine whether the use of vascular resident endothelial progenitor cells to induce therapeutic vascularization in scaffold-based dermal tissue engineering

3.2.3. To evaluate the use of genetically modified dermal fibroblasts expressing VEGF and bFGF to induce therapeutic vascularization a hind limb ischemia model

4. MATERIALS AND METHODS

4.1 Materials and methods related to objective 1

4.1.1 Cell isolation and growth curve

Human sweat gland-derived stem cells (SGSC) were obtained as we described before [15]. Briefly, under a light microscope, sweat glands were mechanically isolated from a predigested and dissociated axillary skin sample. Afterwards sweat glands were cultured in Dulbecco's modified Eagles's medium (DMEM) supplemented with 20% fetal calf serum (FCS) and antibiotics (penicillin 1U/ ml and streptomycin 10 mg/ml) (all purchase from PAA Laboratories, Germany). Medium was replaced every 3 days and cells were split after reaching confluence. After 4 passages, cell propagation was performed in DMEM containing 10% FCS and antibiotics (DMEM-10). Cells (1.5 x 104) were seeded into 6 well plates in triplicates, and DMEM-10 or Endothelial Cell Growth Medium 2, plus suplement mix (EGM; PromoCell, Heidelberg, Germany) was replaced every 3 days. At different time points, cell were trypzinized and counted using an automatic nucleo counter (NC-100, Chemometec, Allerød, Denmark).

4.1.2 Immunocytochemistry

SGSC were cultured on 2-well chamberslides for 48 hours. Then, samples were washed twice with phosphate buffered saline (PBS) and fixed in a solution (7:3) of methanol and acetone containing 1 µg/ ml 4´,6-Diamidin-2-phenylindol (DAPI; Roche, Switzerland) for 5 minutes at 20°C, and rinsed 3 times with PBS. Subsequently, samples were blocked in 1.65% goat serum (Vector Laboratories, CA, USA) for 20 minutes at room

temperature. Primary antibodies against Oct4 (1:100, polyclonal, Santa Cruz, CA, USA), Nanog (1:2000, polyclonal, Chemicon, Germany) and Nestin (1:100, monoclonal, Chemicon) were incubated in a humid chamber over night at 4°C in TBS-T (tris-buffered saline-tritonX: 150 mM NaCl, 10 mM Tris (pH 8,8), 0,05 % tritonX) containing 0.1% bovine serum albumin. Next, samples were washed 3 times with PBS and incubated with Cy3-labeled anti-mouse IgG (1:500, Dianova, Germany) or FITC-labeled anti-rabbit IgG (1:500, Dianova) in a humid chamber for 1 hour at 37°C. Finally, samples were washed 3 times in PBS, mounted in Vectashield mounting medium (Vector Laboratories, CA, USA) and analyzed by fluorescence microscopy (Axioscope 2, Zeiss, Germany). In order to evaluate cell morphology, TRITC-conjugated phalloidin (Sigma-Aldricch, Taufkirchen, Germany) was used according to manufacturer´s intructions.

4.1.3 RNA isolation and RT-PCR

Total RNA isolation was performed according to manufacturer´s instructions using the RNeasy Plus Mini kit (Qiagen, Germany) and the QIAcube for automated RNA isolation including a gDNA removing step. RNA concentration was determined by measuring the absorbance at 260 nm, using a Nanodrop spectrophotometer (Peqlab, Germany). cDNA was synthesized from 500 ng of total RNA using the QuantiTect reverse transcription kit (Qiagen) including a further gDNA digestion step. PCR was carried out with 1 µl cDNA in a 25 µl reaction volume using the QuantiFast SYBR Green PCR kit and QuantiTect Primers (all purchase in Qiagen): Nestin (77 bp), Nanog (90 bp), Octamer binding transcription factor 4 (Oct4; 75 bp), Sex determining region Y-box 2

(Sox2; 64 bp), Krueppel-like factor 4 (Klf4; 72 bp), cMyc (129 bp), Ki67 (86 bp), β3Tubulin (β3T; 78 bp), Protein gene product 9.5 (PGP9.5; 134 bp), Neurofilament (NF; 74 bp), S100 (64 bp), α Smoth Muscle Actin (αSMA; 83 bp), Peroxisome proliferator-activated receptor γ (PPARγ; 113 bp), Runt-related transcription factor 2 (Runx2; 101 bp), Insulin (98 bp), Albumin (106 bp), Amylase (96 bp) and von Willenbrant Factor (vWF; 108 bp). PCR was performed using the Mastercycler ep realplex (Eppendorf, Germany). The amplification cycle included a melting step (95°C) and a combined annealing and amplification step (60°C). Capillar gel electrophoresis was applied on generated PCR-products in the course of the qualitative characterization of mRNA expression. In order to equalise variations in different capillaries, an alignment marker was implemented in every run, and analysis was performed using the BioCalculator software 1.0 (Qiagen). To determine the size of separated DNA fragments, a DNA size marker was used (Qiagen). Finally, results were shown in gel image format.

4.1.4 Scaffold for dermal regeneration and cell seeding

Integra matrix (Integra LifeScience Corporation, NJ, USA) is a scaffold based on bovine collagen fibers cross linked with glycosaminoglycans which forms a porous biodegradable structure. On top, the collagen structure is covered with a removable silicon layer, which acts as a temporal epidermis. Pieces of Integra (6 mm or 12 mm diameter) were dried with sterile gauze, placed in a 24 well plate with the silicon layer facing down. Then, 200 µl of medium containing cells were dropped on each scaffold and quickly absorbed. After 30 minutes of incubation, 1 ml of DMEM-10 was added into each well and medium was

replaced every 2 days. Integra matrix was kindly provided by Integra LifeScience Corporation.

4.1.5 Cytokine array profile and scratch assay

Cells (5 x 105) were seeded and cultured in a piece of scaffold (12 mm diameter). After overnight in culture, medium was replaced for DMEM supplemented with 2% FCS and maintained in culture for another 24 hours. Next, media was removed and cytokine release was evaluated using a cytokine protein array (R&D Systems, Minneapolis, USA), following manufacture´s instructions. Scaffolds without cells were used as negative controls.

SGSC (1 x 104) were seeded in each well of a culture-insert (Ibidi, Martinsried, Germany) in 100 µl DMEM-10. Once the cells reached confluence, inserts were removed and medium was replaced for fresh DMEM-10 or Endothelial Cell Growth Medium 2 (EGM; Promocell, Germany). After 24 hours, pictures were taken and cell migration into the gap area (scratch) was compared and quantified using TScratch software as described before (Gebäck et al., 2009). Results were expressed as the percentage of the original gap surface covered with cells.

4.1.6 Cell visualization in the scaffold and 3-dimensional reconstruction

After seeding for 48 hours, scaffolds containing cells were fixed in 3.7% formaldehyde (Sigma-Aldrich, Taufkirchen, Germany) for 30 minutes at room temperature. Afterwards, the silicon layer was removed and the whole

scaffold was stained for 1 hour with TRITC-conjugated Phalloidin (Sigma-Aldrich), used according to manufacturer instructions. Finally, samples were mounted in ProLong® Gold antifade reagent containing DAPI (Invitrogen, Oregon, USA) and analyzed in an FV10i confocal microscope (Olympus, Hamburg, Germany). Three-dimensional reconstructions were performed using Amira software (Visage imaging GmbH, Berlin, Germany).

4.1.7 Quantification of metabolic activity in the scaffold

Cells (1 x 105) were seeded in a 6 mm diameter scaffolds. At different time points, scaffolds were incubated for 1 hour in fresh medium containing 5 ng/ml of 3-(4,5-dimethyl-2-thiazolyl)-2,5-diphenyl-2H tetrazolium bromide (MTT, Sigma-Aldrich). Next, medium was removed and replaced by 100 µl of dimethyl sulfoxide (DMSO, Sigma-Aldrich). In order to quantify metabolic activity, absorbance at 560 nm was measured in the DMSO containing soluble formazan blue. Scaffolds without cells were used as blank.

4.1.8 Scaffold based dermal regeneration model

Cells (5 x 105) were seeded and cultured in a piece of scaffold (12 mm diameter). After overnight in culture, medium was replaced for DMEM supplemented with 2% FCS and maintained in culture for another 24 hours. Next, media was removed and cytokine release was evaluated using a cytokine protein array (R&D Systems, Minneapolis, USA), following manufacture´s instructions. Scaffolds without cells were used as negative controls.

4.1.9 Quantification of the vascularization levels

In order to quantify vascularization levels, tissue transillumination and digital segmentation was performed as we described before (Egaña et al., 2009). After 2 weeks, skin from the back of the animals was removed and quickly placed over a transilluminator (Hama, LP 5000K, Germany). Then, digital pictures were obtained in TIF format (Olympus camera, C-5060, 5.1 Megapixels) and processed for digital segmentation. For quantification, the percentage of the vascularized area was compared to the normal skin of the same sample (vessel area) and compared among groups. The vessel analysis software used here can be free downloaded at: http://www.isip.uni-luebeck.de/index.php?id=150

4.1.10 Matrigel assay

150 µl of Matrigel (BD bioscience) was added into each well of a 24 well plate and incubated for 1 hour at 37°C. After gelification, 2.5 x 104 SGSC were seeded in each well in EGM or DMEM-10 and pictures were taken after 2h, 5h and 24h. HUVEC cells were used as positive control and cells seeded in polycarbonate as negative control.

4.1.11 Historical analyses

Afterwards, cellurarization levels of the the scaffolds were quantified by analyzing DAPI stained cryosections. Images were acquired with a fluorescence microscope (Axioscope 2, Zeiss, Germany) equipped with different filter sets. With the DAPI channel, nucleic staining was detected and with the FITC channel the autofluorescent integra matrix could be displayed.

Images were obtained using a digital camera (AxioCam MRc5, Zeiss, Germany) with a resolution of 1.3 Megapixel. To calculate the number of DAPI stained nuclei within the matrix an image recognition software was used, which automatically detects the DAPI stained area as well as the integra matrix area (region of interest = ROI), which was defined as a mask. Therefore, a Gaussian blurring was used to get a homogeneous image and to remove details. Then, the ROI was calculated using a threshold based segmentation.
Within these FITC channel masks, cell nuclei were detected using a threshold based segmentation. The number of cells was normalized to the area of the masks, i.e. the number of cells was calculated in cells/ mm2. For these analyses representative microscopy images were used (Control group n= 42; SGSC group n=53). All software development and analysis of this quantification was performed using MATLAB R2010b 64 bit. The histological analysis comprised also an evaluation of the wound bed thickness. Here the area beneath the scaffold was estimated. Wound bed thickness was measured in 24 representative microscopical images per experiment group using the measure tool of the Zeiss Axiovision software.

4.1.12 Statistical analysis

All assays were repeated in at least 3 independent experiments. Data was expressed as mean ± SEM. Two-tailed Student's t-test was used to compare differences between 2 groups. GraphPad Prism 5 software (GraphPad Software, CA, USA) was used for statistic analyses. Differences among means were considered significant when $p<0.05$.

4.2 Materials and methods related to objective 2

4.2.1 Cell isolation and culture

Rat cardiac vascular resident cells were isolated as described before [61, 62]. Briefly, rat heart vasculature was perfused *ex vivo* with Krebs-Ringer buffer containing 0.06% collagenase. Cells were then collected from the recirculation medium and grown under standard cell culture conditions using Dulbecco's Modified Eagle Medium (DMEM) supplemented with 10% Fetal Calf Serum (FCS) and antibiotics (penicillin and streptomycin). Confluent monolayer was split routinely 1:4 after washing with PBS and treatment with trypsin-EDTA. All reagents were purchased from Invitrogen (Karlsruhe, Germany). For clonal analysis, cells were cultured until reaching 80% confluence, detached and sorted by DAKO Cytomation MoFlo High Speed Cell Sorter (DAKO, Denmark). Next, a single cell was placed in a 96 well plate and cell growth was daily examined and counted. After 7 days, only the well with more cells was selected and subcultured for further studies.

4.2.2 Immunocytochemical analysis

Colonized cells were transferred into 2 well chamber slides (Becton Dickinson GmbH, Heidelberg, Germany) and cultured until sub-confluence. Then, cells were fixed for 10 minutes in 5% paraformaldehyde (PFA) containing 1 µg/ml 4',6-diamidino-2-phenylindole (DAPI; Roche Molecular Biochemicals, Mannheim, Germany) at room temperature and washed 3 times in phosphate buffered saline (PBS). Next, samples were blocked for 20 minutes in 1.65 % normal goat serum at room temperature. Specimens were incubated with primary antibodies for 1 hour our at 37°C in a humid chamber. Here we used

antibodies against Nestin (mouse monoclonal, 1:250, Abcam, Cambridge, UK), Neurofilament H (NF-H, rabbit polyclonal, 1:500, Serotec, Kidlington, UK), Troponin I Typ 1 (mouse monoclonal, 1:50, Acris, Herford, Germany), and GATA4 (mouse monoclonal, 1:100, Santa Cruz Biotechnology, Santa Cruz, USA). After rinsing 3 times with PBS, slides were incubated for 1 hour at 37°C with Cy3-labelled anti-mouse IgG (1:400) and FITC-labeled anti-rabbit IgG (1:200) (both purchase from Dianova, Hamburg, Germany). Then, slides were washed 3 times in PBS, covered in Vectashield mounting medium (Axxora, Grünberg, Germany) and analyzed with a fluorescence microscope (Axioskop Zeiss, Göttingen, Germany). Images were captured with the axiovision software (Zeiss, Göttingen, Germany) and fluorescence intensity was normalized to a black background. All immunocytochemical results showed typical morphologic features corresponding to targeted cellular structures, indicating a specific staining of these antibodies. The negative controls were carried out with the secondary antibodies alone and showed only unspecific faint staining (data not shown).

4.2.3 Real-Time PCR analysis

Total cellular RNA was isolated using the RNeasy Plus Mini Kit (Qiagen, Hilden, Germany) and a robotic workstation for the purification of RNA (QIAcube, Qiagen, Hilden, Germany). RNA concentration was determined by measuring the absorbance at 260 nm and 0.5 µg of total RNA was reverse transcribed into cDNA using QuantiTect reverse transcription kit (Qiagen, Hilden, Germany) according to the manufacturer's instructions. The quantitative real-time PCR (qRT-PCR) was performed with 1 µl cDNA in a 25 µl reaction volume using the

QuantiTect SYBR Green PCR Kit and QuantiTect Primers (α-Actin: Rn_Acta2_1_SG, amplicon length: 82 bp; DMC1: GATA4: Rn_Gata4_1_SG, amplicon length: 70 bp; GFAP: Rn_Gfap_1_SG, amplicon length: 131 bp; Nestin: Rn_Nes_1_SG, amplicon length: 63 bp; Neurofilament L: RnNefl_1_SG, amplicon length: 69 bp; Oct-4: Rn_Pou5f_1_SG, amplicon length: 134; Troponin I Typ 1: Rn_Tnni1_1_SG, amplicon length: 137 bp: Von Willebrandt Factor: Rn_Vwf_1_SG, amplicon length: 107 bp (all Qiagen, Hilden, Germany). The amplification cycles were performed with the Mastercycler ep realplex (Eppendorf, Hamburg, Germany) and included a melting step (95°C) and a combined annealing and amplification step (60°C). All quantifications were performed in triplets. Automated gel electrophoresis was carried out with the QIAxcel capillary gel electrophoresis system (Qiagen, Hilden, Germany).

4.2.4 *In vitro* cell differentiation assay

For adipogenic or osteogenic differentiation cells were cultured in differentiation medium containing adipogenic supplements (hMSC Differentiation BulletKit ®–Adipogenic, Lonza, Cologne, Germany) or osteogenic supplements (hMSC Differentiation BulletKit ®–Osteogenic, Lonza, Cologne, Germany) according to manufacture's instructions. Tube formation assay was performed described before [31]. After differentiation, Oil red O staining (Invitrogen, Oregon, USA) and Von Kossa staining (Polysciences Europe GmbH, Eppelheim, Germany) were performed. Mouse pancreatic stem cells (PSC) were used as positive controls.

4.2.5 Scaffold for dermal regeneration and cell seeding

Integra matrix (IM) is a scaffold based on bovine tendon collagen fibers cross linked with glycosaminoglycans which forms a porous biodegradable structure. On top, the collagen structure is covered with a removable silicon layer, which acts as a temporary epidermis. Pieces of IM (12 mm diameter) were dried with sterile gauze and placed in a 24 well plate, and then 300 μl of medium containing $1x10^6$ cells were dropped over the scaffold being quickly absorbed for it. After 30 minutes of incubation, 1 ml of DMEM+10% FCS was added into each well. Cell seeding efficiency was evaluated by removing the scaffold from the well and counting cells adhered to the culture dish. IM was kindly provided by Integra LifeScience Corporation, NJ, USA.

4.2.6 Cell visualization in the scaffold

After seeding for 14 days, Integra matrix containing cells was fixed in 3.7% paraformaldehyde (PFA, Sigma-Aldrich, Taufkirchen, Germany) for 30 minutes at room temperature (RT). Scaffolds were then permeabilized with 0.2% Triton for 30 minutes and stained for 1 hour with TRITC-conjugated phalloidin (Sigma-Aldrich) at RT. Finally, samples were mounted in prolong anti-fade containing DAPI (Invitrogen, Oregon, USA) and analyzed by an FV10i confocal microscope (Olympus, Hamburg, Germany). For 3-dimensional view of the scaffold, slices from Z-axis were reconstructed by Amira 4.0 software (Visage Imaging GmbH, Berlin, Germany).

4.2.7 Quantification of metabolic activity in the scaffold

Cells ($1x10^6$) were seeded into each scaffold (12 mm of diameter) in 1 ml DMEM + 10% FCS. At days 1, 7 and 14 after seeding, medium was removed

and scaffolds were incubated for 1 hour in fresh medium containing 5 ng/ml MTT (Sigma-Aldrich, Taufkirchen, Germany). After incubation, medium was replaced by 500 μl dimethyl sulfoxide (DMSO; Sigma-Aldrich). In order to quantify metabolic activity, absorbance at 570 nm was measured in the DMSO containing soluble formazan blue. Scaffolds without cells were used as negative control.

4.2.8 Scaffold-based dermal regeneration model

Scaffolds obtained from 9 athymic nude mice (6-8 weeks old; Taconic, Copenhagen, Denmark) were analyzed. Animals were distributed in 2 groups: 4 controls (8 empty scaffolds, 2 scaffolds per animal) and 5 animals containing VR-EPCs (10 cell-seeded scaffolds). Before transplantation animals were anesthetized with ketamine (10 mg/kg) and xylazin (2.4 mg/kg) via intraperitoneal injection. Under general anesthesia, a bilateral full skin defect was created (10 mm diameter) in the back of the animals and the skin was replaced by control (empty) or cell-seeded scaffolds (Figure. 24). In order to minimize possible artifacts during tissue harvesting, a titanized mesh (TIMESH, GfE Medizintechnik GmbH, Germany) was placed between the wound bed and scaffolds. Scaffolds were fixed to the wound by using non-absorbable sutures and wounds were bandaged with sterile gauze. Two weeks after transplantation, animals were sacrificed by overdose of ketamine/ xylazin and the scaffolds were removed for further analyses. All procedures *in vivo* were approved by the corresponding local ethical committees.

4.2.9 Scaffold vessel visualization and quantification

In order to quantify vascularization levels, tissue transillumination and digital segmentation were performed. After 2 weeks, skin from the back of the animals was removed and quickly placed over a transilluminator (Hama, LP 5000 K, Germany), digital pictures were obtained in TIF format (Olympus camera, C-5060, 5.1 Megapixels) and then processed for digital segmentation. Results were expressed as percentage of vascularization (vessel area and vessel length) compared to normal skin as described before[63]. The vessel analysis software used here can be downloaded at: http://www.isip.uni-luebeck.de/index.php?id=610.

4.2.10 Histology analysis

In order to analyze the density and distribution of cells and vessels in the implanted scaffolds, histological analyses were performed with hematoxylin and eosin (HE) and DAPI staining. Two weeks after implantation scaffolds were harvested, fixed with 3.7 % PFA for 1 hour, dehydrated, and embedded in paraffin. 10 μm thick paraffin sections were obtained from the center of the scaffold, deparaffinized and stained with standard HE and DAPI staining protocols. Functional blood vessels were identified by morphology and the presence of erythrocytes inside the vessel wall. Vessel number was obtained by counting on at least 3 different sections which were located at least 100 μm far of each other. Cellularization was evaluated in the border zone, defined by counting the cell number in 3 different areas (20X pictures) of each section in the cell infiltration zone which was defined by 0 μ m to 240 μ m (white dot line in Figure 26B) above the border (red dot line in Figure 26B) between the scaffold and the wound bed. All histological results were obtained by 2

independent researchers.

4.2.11 *In vitro* tube formation assay

VR-EPCs were cultured on polystyrene surface or Matrigel™ (BD Biosciences, USA) coated surfaces in DMEM + 10% FCS or in Endothelial Cell Growth Medium 2 (EGM) with supplement mix (PromoCell, Heidelberg, Germany). Matrigel was added into 48 well culture plates and allowed jellifying at 37℃ for 30 minutes. Next, 5 x 10^3 cells, in 0.5 ml medium, were added on top of the matrigel coated surface. After 1 day, cells were fixed with 3.7 % PFA and stained with TRITC-conjuncted Phalloidin (Sigma-Aldrich, Munich, Germany) and DAPI (Invitrogen, Oregon, USA). Quantification was evaluated by counting the number of tubes per field in 3 different random areas of each well.

4.2.12 *In vitro* cell migration assay

VR-EPCs (1 x 10^4) were seeded in a Culture-Insert (Ibidi, Martinsried, Germany) in 100 µl DMEM + 10% FCS. Once the cells reached confluence, the insert was removed and medium was replaced by fresh DMEM + 10% FCS or Endothelial Cell Growth Medium 2 (EGM; PromoCell, Germany). After 10 hours, pictures were taken and cell migration in the open wound area (no cell covered area labeled in grey) was compared and quantified using TScratch as described before [64]. Results were obtained from 3 representative pictures of each well in 3 independent experiments and were expressed as open wound area (10 hour) percentages of the open wound area (0 hour).

4.2.13 *In vitro* cytokine antibody profiling

VR-EPCs (5 x 10^6 cells) were seeded in 75 cm^2 culture flasks with DMEM + 10% FCS. After overnight incubation, medium was replaced for DMEM + 2% FCS and maintained in culture for another 72 hours. Next, medium was collected and cytokine release was evaluated with a RayBio® Rat Cytokine Antibody Array 2 (RayBiotech, Georgia, USA) used according to manufacturer's instructions.

4.2.14 Statistical analysis

All cell culture and biochemical analyses were repeated in at least 3 independent experiments. Data are shown as mean ± SEM. Statistical comparisons between 2 groups were performed with two-tailed Student's t-test. Multiple comparisons between groups were applied when necessary with one way ANOVA followed by post hoc analysis. Differences among means were considered significant when $p<0.05$.

4.3 Materials and methods related to objective 3

4.3.1 Rat dermal fibroblasts isolation and characterization

Fibroblasts were isolated from skin obtained from the back of inbred rats. Briefly, the samples were cut into 4 cm x 1 mm strips and then incubated with Dispase-2 (Roche, Penzberg, Germany). Subsequently, the epidermal layer was carefully removed and the dermis was minced and then incubated for 3 hours under magnetic rotation with 0.1% collagenase (Roche, Penzberg, Germany). After that, the mixture was filtered through a 100-µm Cell Strainer (BD biosciences, Hamburg, Germany) to obtain the primary cells. For characterization, cytospinned cells and normal cells seeded for 48 hours were

fixed in ice-cooled ethanol for 30 minutes. Subsequently, the cells were stained with anti fibroblast antibody (Prolyl 4-hydroxylase subunit beta: P4H beta, Acris, Heidelberg, Germany) and tetramethyl rhodamine isothiocyanate conjugated phalloidin (Sigma-Aldrich, MO, USA) according to the manufacturer's instructions. Then, the cells were mounted in Prolong-containing DAPI (Invitrogen, Oregon, USA). Afterwards, cell morphology was analyzed by phase-contrast /fluorescence microscopy (Nikon, eclipse te2000-s).

4.3.2 High-efficient ex vivo nucleofection

Nucleofection was performed under different conditions, and 1 x 10^6 primary rat skin fibroblasts (passage 2, 80–90% confluent) were trypsinized and harvested by centrifugation at 100xg for 10 min. The original nucleofection protocol was conducted following the suggested instructions (Basic Primary Mammalian Fibroblast Nucleofector® Kit , Lonza, Cologne, Germany). The supernatant was removed and the cell pellets were resuspended in 100 µl of nucleofection solution or 100 µl of Dulbecco's Modified Eagle Medium(DMEM) supplemented with 10% Fetal Calf Serum (FCS) for the purpose of comparing different nucleofection solutions. Afterwards, 4 µg of pmaxGFP® plasmids (Lonza) were mixed with the cells and subsequently transferred into nucleofection cuvettes. We also tested different transfection cuvettes and found that Eppendorf electroporation cuvettes (4-mm gap, Eppendorf, Hamburg, Germany) were as efficient as Amaxa cuvettes（2-mm gap, Amaxa, Cologne, Germany）. Subsequently, the cells were nucleofected by using the U30 program from the nucleofection device and 500 µl of pre-warmed culture medium was immediately added to the cells. The cells were trypsinized and

analyzed with a CASY® system (Innovatis AG, Reutlingen, Germany) for cell number and cell viability 48 hours after transfection. Transfection efficiency and apoptosis were quantified by fluorescent activated cell sorting (FACS; Cytomation MoFlo® Flow Cytometer, Dako, Denmark). DMEM + 10% FCS, Eppendorf cuvettes (4-mm gap, Eppendorf, Hamburg, Germany) and U30 program were chosen for the *in vitro* and *in vivo* study. Plasmids encoding for VEGF165 and bFGF were constructed based on pmaxGFP® backbone (Lonza). The modified VEGF165 nucleofection protocol was as following: 1) Fibroblasts (3×10^6, passage 2) were mixed with 12 µg of VEGF165 plasmid and 100 µl of nucleofection solution (DMEM + 10% FCS); 2) the mixture was then transferred into Eppendorf electroporation cuvettes (4-mm gap) and nucleofected with single electropulse program U30. After that, cells were transferred into a T25 culture flask and 4 ml DMEM+10% FCS were added; 3) the above two steps were repeated for 5 times with a total of 15 x 10^6 cells. 4) After 24 hours, VEGF165 nucleofected cells were collected and counted, only 5 x 10^6 cells were obtained for *in vivo* administration. The bFGF nucleofection protocol was conducted at the same time as VEGF165 nucleofection with another 15 x 10^6 cells to obtain 5 x 10^6 bFGF nucleofected cells. Cells (5 x $10^6$with bFGF and 5 x 10^6 with VEGF165) were then mixed before *in vivo* cell administration.

4.3.3 Growth-factor production

Transfected cells (1.4 x 105) were seeded in 12-well plates and cultured in 1.5 ml of DMEM + 10% FCS. Subsequently, medium was changed and collected daily. Concentrations of VEGF165 and bFGF were quantified by Bio-Plex

Suspension Array System, following manufacturer's instructions (Bio-Rad, Hamburg, Germany).

4.3.4 Hindlimb ischemia model

Experiments were performed on male Lewis inbred rats (weight 200 grams, Charles River Laboratories, Sulzfeld, Germany). Femoral artery ligation was performed as described previously [65]. All *in vivo* procedures were approved by animal committee of Luebeck University (No.1/1m/09).

4.3.5 Cell administration

Animals were randomly divided into 2 groups of treated and control animals. Directly after ligation of the right femoral artery, the cells (1X107) transfected with VEGF165 or bFGF (5 x 106 each) were intramuscularly injected into the gracilis muscle and adductor muscles in the middle part of the thigh because it has been demonstrated that this is the site of major collateral growth in the rat model employed but also in other animal models [65, 66]. This is also the site of major collateral growth in humans when the superficial femoral artery is occluded and was consequently chosen as main injection site in the TAMARIS and WALK trials [67]. The same number of cells without transfection was injected into the same site in control group.

4.3.6 Quantitative micro-CT system

High-resolution desktop X-ray micro-CT system (SkyScan1072, SkyScan, Belgium) was used to visualize and quantify the vascular networks. Seven days after femoral artery ligation, micro-CT angiographies were performed as

described before with modifications [65], After perfusion with the contrast medium, the ischemic zone of limbs was reconstructed from Z-axis cross section slices. After visualization and reconstruction of the vascular networks in the ischemic zone, collateral vessels were quantified and compared between the control and treated animals as described earlier [65]. Typical corkscrew-like collateral vessels were counted in 3D view. Compared to X-ray view, collaterals were easier to identify. After 3D reconstructions, the bone structures were subtracted and the vessel volume was quantified. Voxel number information from reconstruction slices of the ischemia zone (600 cross-sections below the proximal end of the ligation point) was collected for quantification of blood volume.

4.3.7 Plasmid pharmacokinetics

The distribution of the plasmid was assessed by real-time PCR detecting the pmaxGFP® plasmid backbone sequences. At day 3, 7, 14, and 28 after injections, animals were sacrificed and organs were carefully collected and frozen for plasmid detection. Afterwards, the DNA was isolated with NucleoSpin® Tissue kit (MACHEREY-NAGEL, Dueren, Germany) and detected with specific primer for the plasmid backbone.

4.3.8 Local gene expression

Seven days post injection, animals were sacrificed and samples were obtained from the muscles of the treated and control animals. Total RNA was then isolated with NucleoSpin® RNA II kit (MACHEREY-NAGEL, Dueren, Germany) according to the manufacturer's instructions. VEGF165 and bFGF mRNA

expression was detected with specific primer for both the genes.

4.3.9 Collateral proliferation and blood perfusion ratio

Animals were sacrificed, the middle zone of the collaterals on day 7 including the surrounding tissues were taken, and proliferation assays were performed as described previously [68]. Proliferation of the collateral artery was detected by 5-Bromo-2'-Deoxyuridine (BrdU) labeling and detection Kit 2 (Roche Diagnostics, Penzberg, Germany). The proliferative index was calculated as the number of BrdU-positive nuclei to the total number of nuclei inside the vessel wall. Blood flow in the lower hindlimb was detected on day 7 after ligation by FluoSpheres polystyrene microspheres (15 μm, red-fluorescent, Invitrogen, USA). The microspheres were injected via catheters through the carotid artery of rats running on a treadmill. After injection, rats were sacrificed and gastrocnemius and soleus from both hindlimbs were taken. Blood flow was expressed as ratios of occluded and non-occluded hindlimb perfusion (microspheres numbers) of the soleus and gastrocnemius.

4.3.10 Statistical analysis

All data were evaluated by at least 3 independent experiments. The data were shown as Mean ± SEM. Statistical comparisons between 2 groups were performed with two-tail Student's t-test. One-way ANOVA followed by post-hoc analyses was used for comparison of differences within multiple groups. The differences between the groups were considered significant when $p<0.05$.

5. RESULTS

5.1 Results from objective 1

5.1.1 Stem cell characterization

Sweat gland-derived stem cells (SGSC) were isolated and characterized. Here we found that cells adhere to polystyrene, showing fibroblast-like morphology (Figure. 8a) and a high proliferation rate with a doubling time of about 4.3 days (Figure. 8b). In order to determine the expression of stem cell markers and to evaluate their multilineage differentiation potential *in vitro*, immunocytochemistry was performed. Results showed that SGSC express Oct4, Nestin and Nanog (Figure. 8c). Furhermore, RT-PCR showed the expression of stem cell and differentiation markers. Here we have found that, in addition to Oct4, Nestin and Nanog, SGSC also express the stem cell markers Sox2, Klf4 and cMyc. Furthermore, we found that cells also expressed the proliferation marker Ki67 and, due to their spontaneous differentiation *in vitro*, we detected transcripts of cells derived from the Ectoderm (ß3T, PGP9.5, NF, S100), Mesoderm (αSMA, PPARγ, Runx2) and Endoderm, (Albumin, Amylase, vWF) (Figure. 8d). Next, the functional effects of pro-angiogenic environments on the behavior of SGSC were evaluated. Here we have found that when cells were seeded on Matrigel coated surfaces, they acquire an endothelial-like behavior, thus forming capillary-like structures in DMEM-10 and endothelial growth medium (EGM) (Figure. 9a). Further we have also found that EGM increased cell migration, evaluated in a scratch assay, (Figure. 9b; $p < 0.001$), and induced cell proliferation (Figure. 9c; $p < 0.05$).

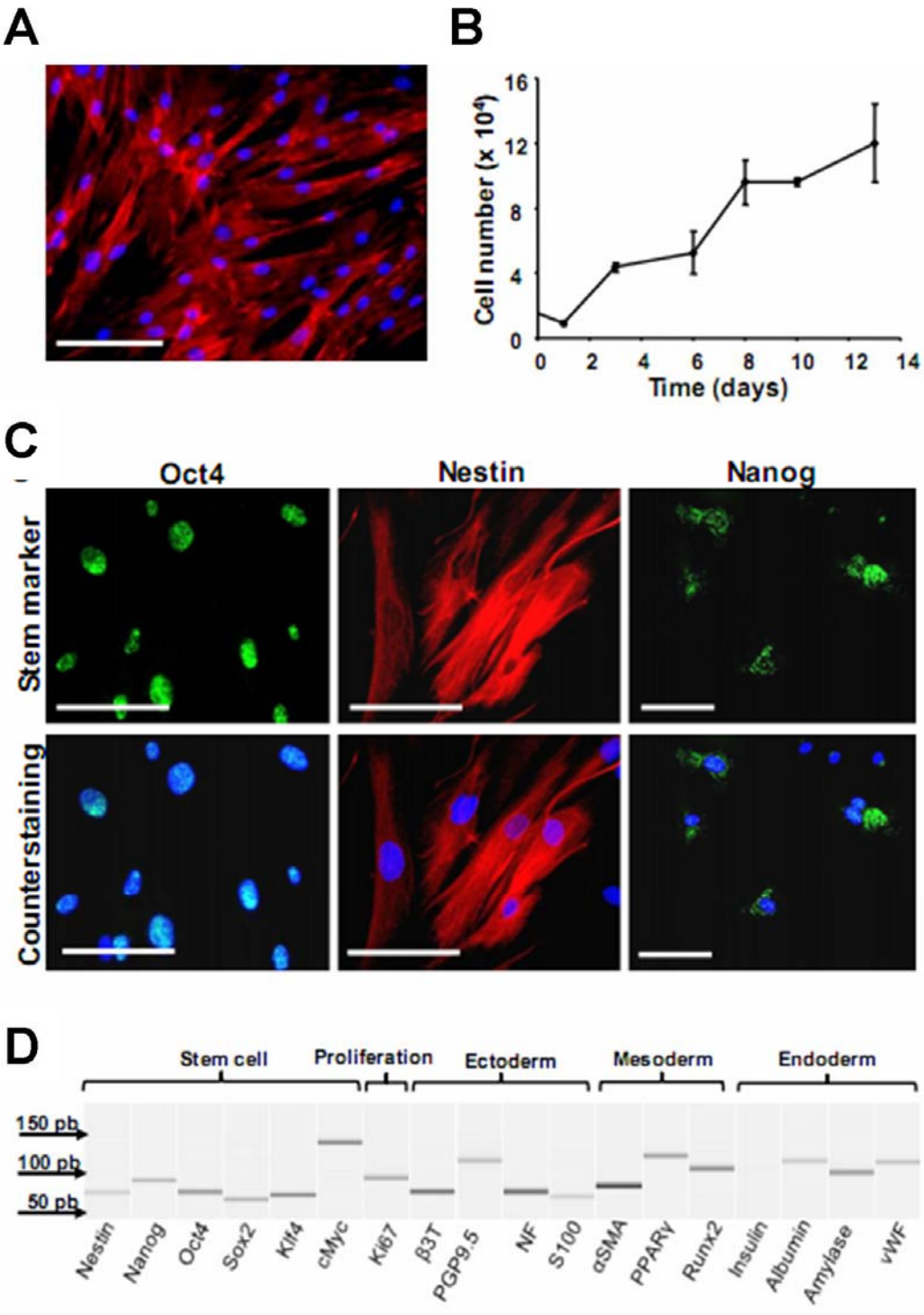

Figure 8: Characterization of sweat gland-derived stem cells. Cells were isolated and characterized in terms of morphology (A), proliferation capacity (B) and the presence of the stem cell markers Oct4, Nestin and Nanog, all counterstained with DAPI (C). RT-PCR analysis showed the expression of the stem cell markers Nestin, Nanog, Oct4, Sox2, Klf4 and, cMyc (D). In addition, cells expressed the proliferation marker Ki67 and differentiation markers of cells derived from the Ectoderm (ß3T, PGP9.5, NF and, S100), Mesoderm (αSMA, PPARγ and Runx2) and Endoderm (Albumin, Amylase and, vWF). Scale bar represent 100 µm.

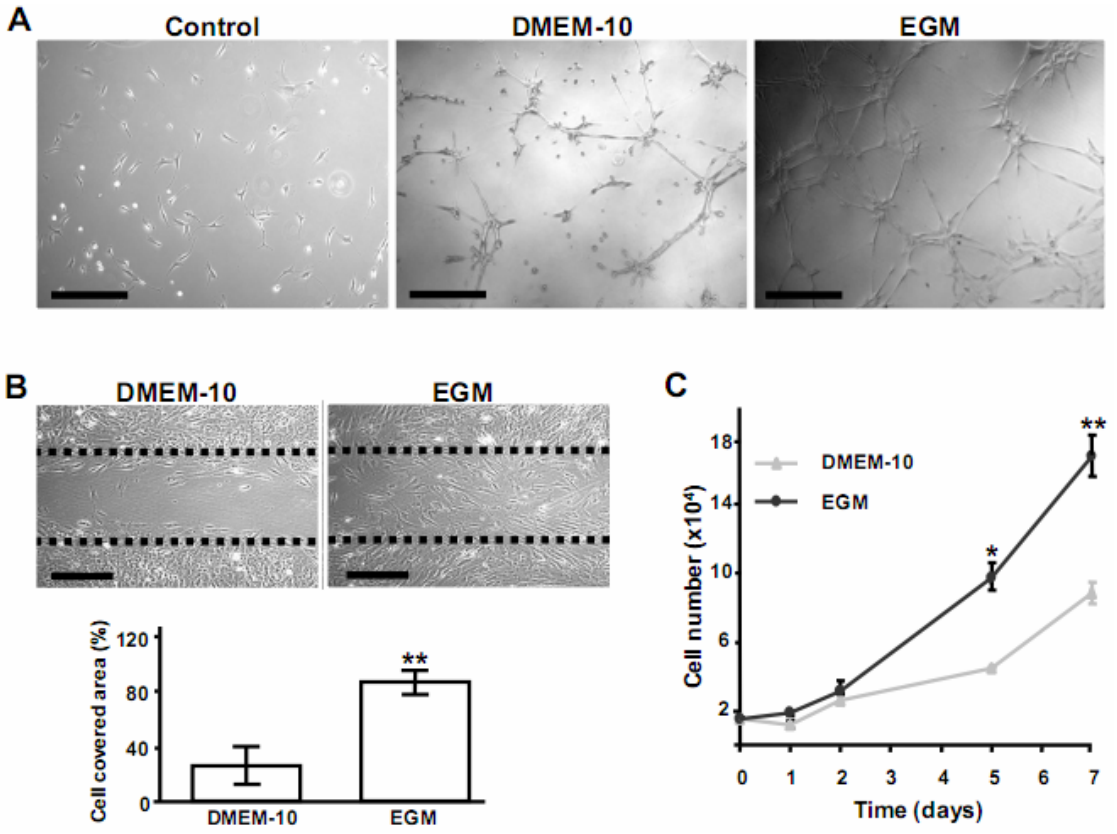

Figure 9: Behavior of sweat gland-derived stem cells in angiogenic environments. Cells were seeded on polycarbonate (control) or matrigel coated surfaces. Results show that cells formed capillary like structures in both DMEM-10 and EGM (A; n=3). In addition, cell migration (B; n=9) and proliferation (C) were significantly increased in EGM compared to DMEM-10. Scale bar represents 50 µm in A and 300 µm in B. *p < 0.05; **p < 0.001. Results are presented as mean ± SEM.

5.1.2 Distribution and viability of cells in the scaffold after seeding

After seeding in the scaffolds, cells were stained and analyzed by confocal microscopy. Here homogeneous distribution and direct attachment of the cells to the collagen scaffold were observed (Figure 10a). Afterwards, viability of the SGSC was determined by metabolic MTT assays. Results showed that in the presence of MTT scaffolds containing cells become dark-blue. As shown in figure 10b, such color was homogeneously distributed showing that, for at least 14 days after seeding, cells were metabolically active in all areas of the scaffold. Moreover, a significant increase in metabolic activity from day 1 to

day 14 suggests cell proliferation in the scaffold ($p < 0.05$). In order to evaluate the release of bioactive molecules from cell seeded scaffolds, a cytokine array profile was performed. Results showed that scaffolds containing cells were able to release several bioactive molecules, which are involved in key processes for tissue regeneration such as angiogenesis, immune response and tissue remodeling. Here we detect the presence of PAI-1, MMP-9, TIMP-1, PTX3, TSP-1, uPA, VEGF, CD26, Ang, IGFBP-3 and IL-8 (Figure 10c). The next molecules were either not detected or detected in very low levels: Activin A, ADAMTS-1, Angiopoietins 1, Angiopoietins 2, Angiotastin, Amphiregulin, Artemin, Coagulation factor III, CXCL16, EGF, EG-VEGF, Endoglin, Endostatin, Endothelin-1, FGF acidic, FGF basic, FGF-4, FGF-7, GDNF, GM-CSF, HB-EGF, HGF, IGFBP-1, IGFBP-2, IL-1β, TGF- β1, Leptin, MCP-1, MIP-1α, MMP-8, NRG1-β1, PD-ECGF, PDGF-AA, PDGF-BB/ AB, Persephin, CXCL4, PlGF, Prolactin, Serpin B5, Serpin F1, TIMP-4, TSP-2, Vasohibin and VEGF-C.

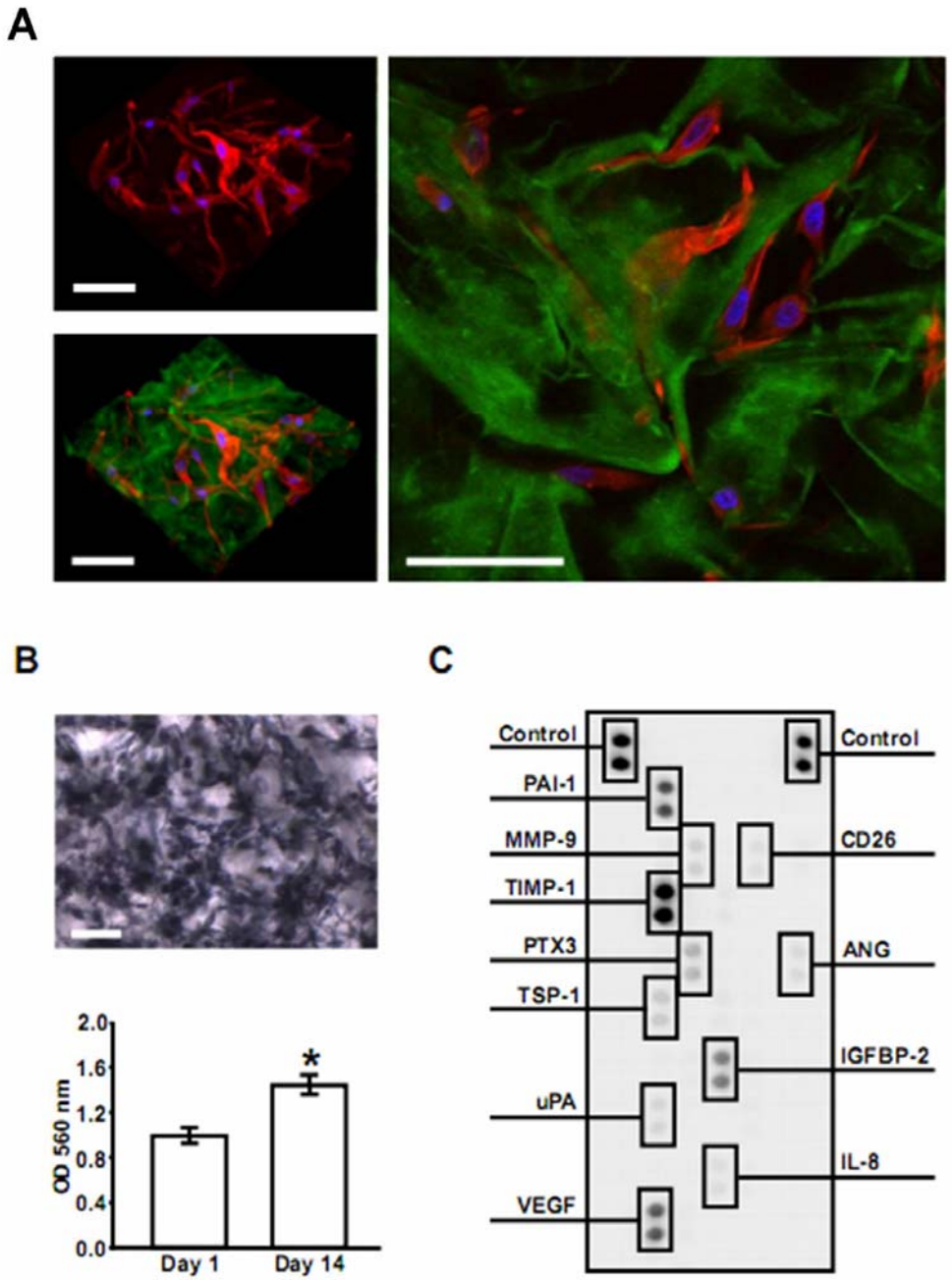

Figure 10: Cell seeded scaffolds. After seeding in the scaffold, distribution and interaction of the cells was analyzed. A 3-dimensional reconstruction of the seeded scaffold is shown in a. Here cells are presented in blue (DNA: DAPI) and red (f-actin: phalloidin) and the scaffold in green (autofluorescence). Homogeneous distribution (A, left) and direct interaction of SGSC to the scaffold was observed (A). Cell metabolic activity in the scaffold was evaluated for 14 days by MTT assay. Results showed the seeded scaffolds turn to dark-blue in the presence of MTT (B, upper). Moreover, an increase in metabolic activity was observed after 14 days in culture (*$p < 0.05$; n=3). After 24 hours, conditioned mediums were collected and the presence of several bioactive molecules was detected. (C) In contrast to non-seeded scaffolds, medium from SGSC-seeded scaffolds contain: PAI-1, MMP-9, TIMP-1, PTX3, TSP-1, uPA, VEGF, CD26, Ang, IGFBP-2 and IL-8. Scale bar represents 100 µm. Results are presented as mean ± SEM.

5.1.3 Induction of vascularization *in vivo*

After confirming that SGSC can be used to bioactivate scaffolds for dermal regeneration, scaffolds were engrafted in an *in vivo* full skin defect model (Figure. 11). Here scaffolds containing cells were well tolerated by the animals and no evident side effects were observed in either group. In order to quantify the influence of SGSC in the vascularization process, animals were sacrificed 2 weeks after engraftment and the whole skin from the back, including the scaffolds, was removed. Afterwards, vascularization levels were quantified by tissue transillumination and digital segmentation. Compared to controls (non seeded scaffolds), a much more widespread vascular network throughout the whole scaffold was observed in the presence of SGSC (Figure 12a). Quantification of the vascularized area showed significant differences between cell-seeded scaffolds and the control group (Figure 12a; $p < 0.001$), with values of 62.28% 8.6% for control and 95.6 % 10% (mean SEM; n=8) for the scaffolds containing SGSC. Afterwards, scaffolds were subjected to histological analysis and their general structure and cellularization level was evaluated (Figure 12b). Here we found that the tissue directly beneath the scaffold was significantly thicker in the group containing SGSC (Figure 12b; $p < 0.005$). Unexpectedly, the presence of SGSC decreased the cellularization levels of the scaffold (Figure 12b; $p < 0.001$).

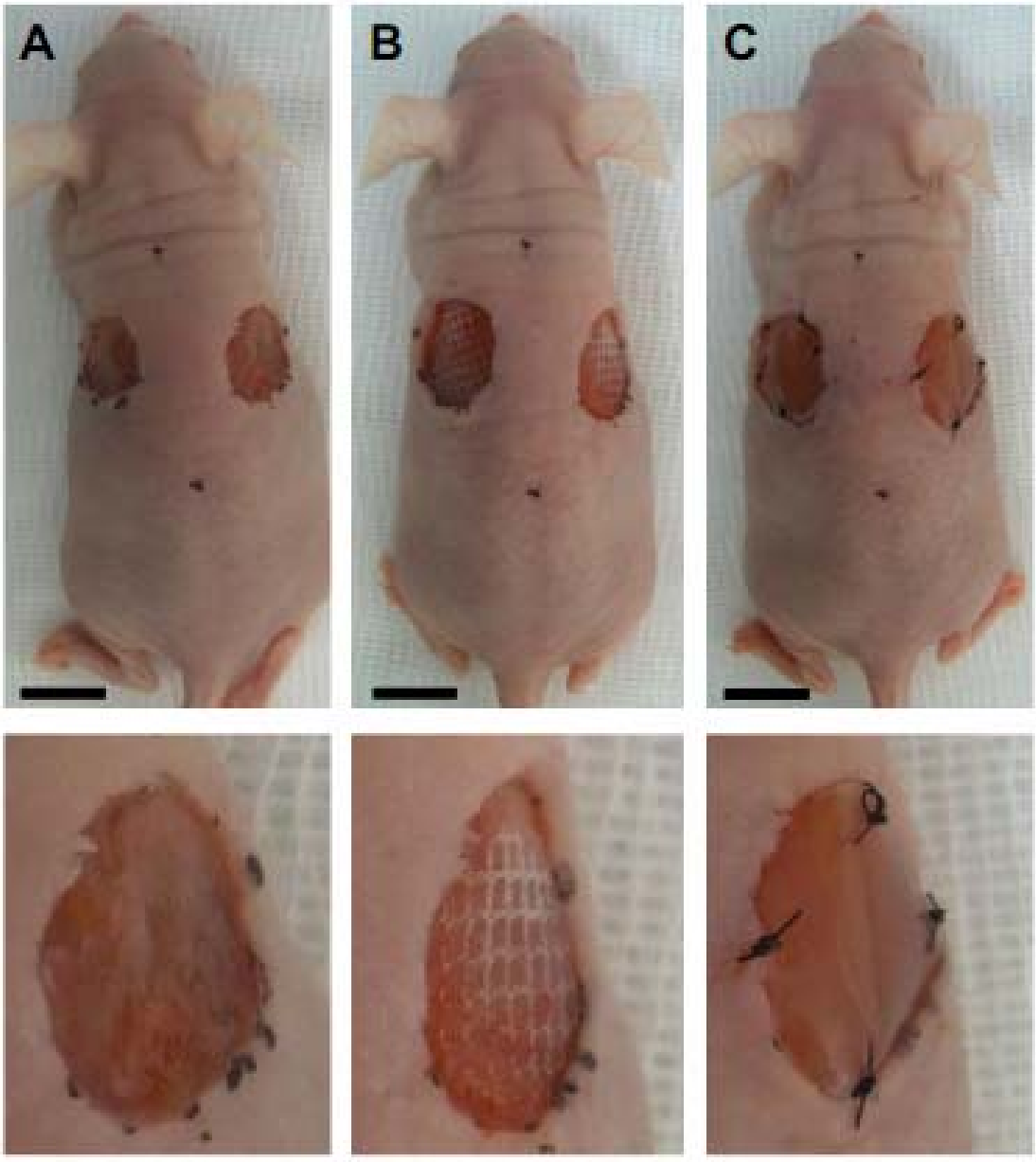

Figure 11: Bilateral full skin dermal regeneration model. A 10 mm diameter bilateral full skin defect was created in the back of the animal (A). In order to avoid contraction of the wound and to minimize artifacts during tissue harvesting, a titanized mesh was placed between the wound bed and the scaffold (B). Finally, the wound was covered with a scaffold for dermal regeneration (C). Lower panel shows the wound area in higher magnifications. Scale bar represents 10 mm.

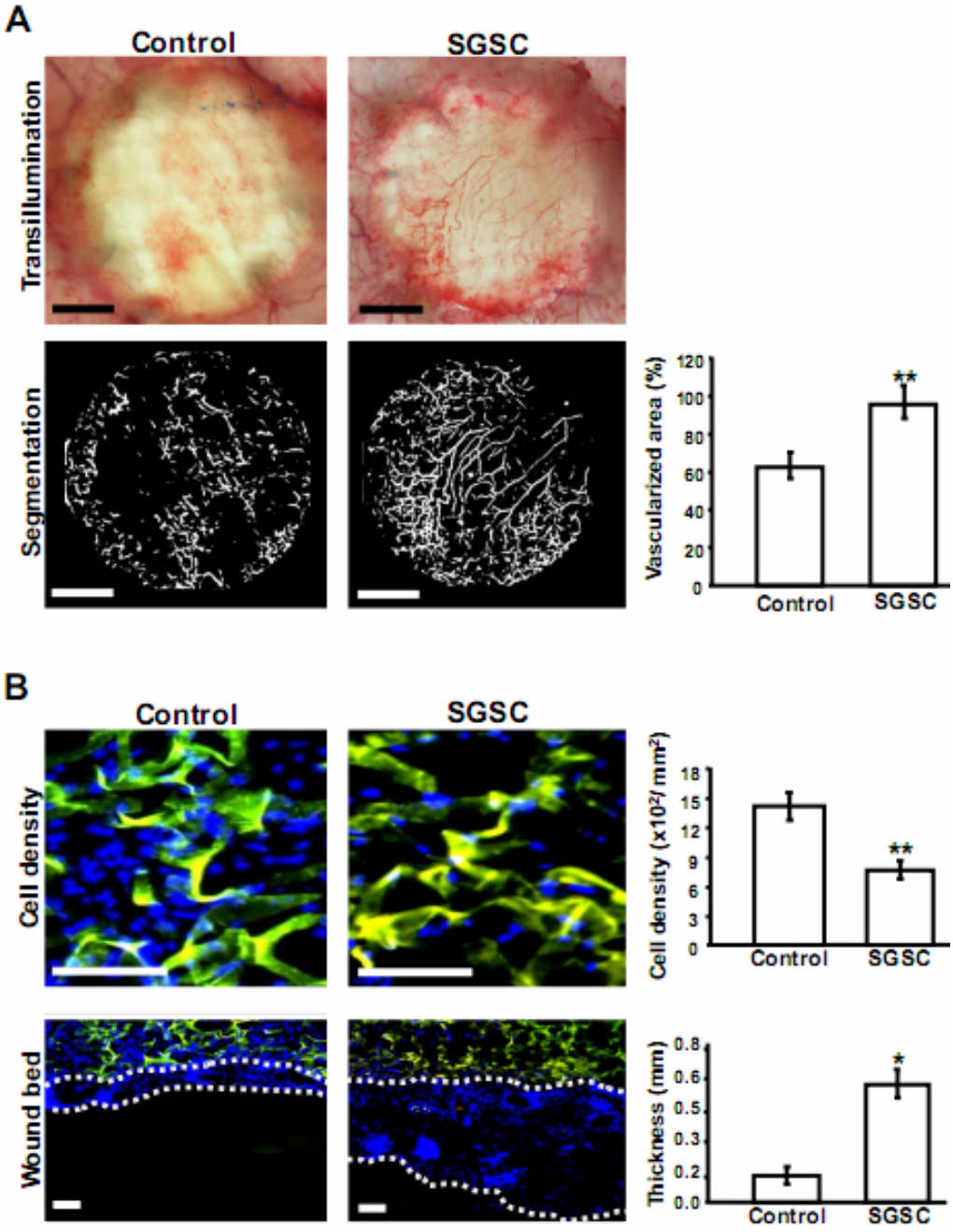

Figure 12: Vascularization and structure of the scaffolds *in vivo*. Two weeks post transplantation, Vascularization levels and the general structure of the wound were analyzed and compared. A representative picture of each group is shown by transillumination and digital segmentation (A). Quantification of the vessel area from control (non-seeded scaffold) or scaffold containing sweat gland-derived stem cells (SGSC) showed significantly higher vascularization in the presence of SGSC (A). Histological analysis shows that the presence of SGSC decreased the cellularization levels (DAPI: blue) of the scaffolds (autofluorescence: green), and increases the thickness of the wound bed (B). Results are representative of 8 independent scaffolds per group. Scale bar represents 200 µm in a and 100 µm in b. *p < 0.05; **p < 0.001. Results are presented as mean ± SEM.

5.2 Results from objective 2

5.2.1 Cell characterization and differentiation

By selection for clonogenic cells, we were able to isolate one cell line which could be cultured for more than 100 passages. When seeded on polystyrene surfaces cells were adherent, showing a cobblestone like morphology (Figure 13 left) and a high proliferation capacity, with a doubling time of about 18 hours (Figure 13 right). The expression of stem and differentiation markers was evaluated by immunocytochemistry and RT-PCR. Immunocytochemical analyses showed the expression of stem cell marker nestin and differentiation markers from cells derived from the 3 different germal layers including: Neurofilament (ectodermal); Troponin I type 1 (mesodermal) and GATA4 (endodermal) (Figure 14A). RNA expression analyses showed the expression of stem cell markers (Nestin and Oct-4) and markers for multilineage differentiation including: Glial fibrilary acidic protein (GFAP); Neurofilament (NF); Troponin I type 1(TNNI 1); α-Smooth muscle actin (α-SMA); Von Willebrand factor (vWF) and GATA4 (Figure 14B). After, we decided to evaluate the behavior of VR-EPCs when cultured under differentiation conditions [69]. First we evaluated the capacity of the cells for differentiating into adipocytes and osteoblasts after seeding under standard differentiation conditions. In contrast to pancreatic stem cells (PSC), the formation of fat vacuoles and the presence of calcium precipitates were not observed in VR-EPC. However both cell types, PSC and VR-EPCs, formed capillary like structures on matrigel coated surfaces (Figure 14C).

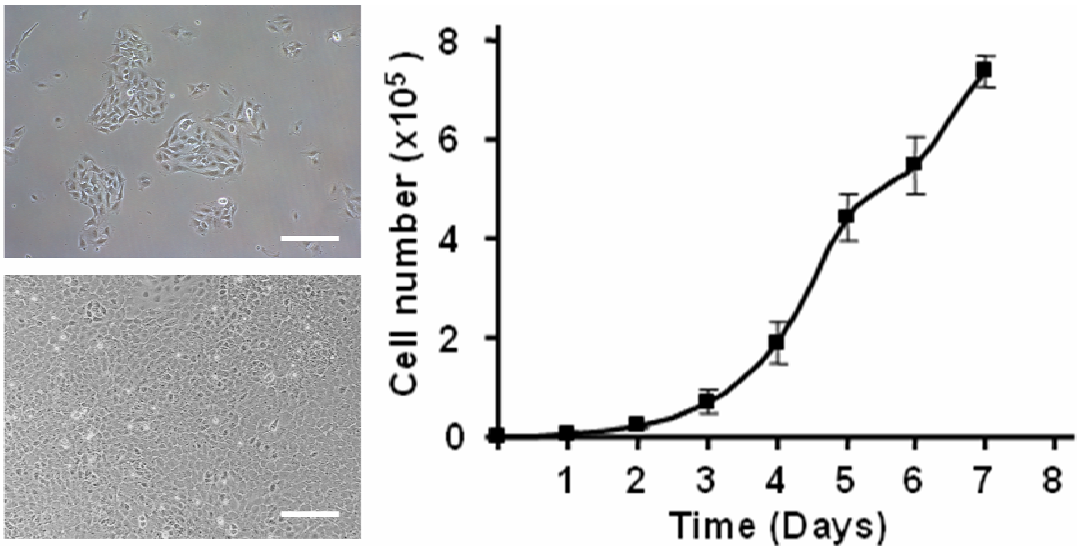

Figure 13: VREPCs characterization. When cultured in DMEM supplemented with 10% FCS, VR-EPCs were strongly adherent to polycarbonate, showing a cobblestone like morphology (left) and high proliferation capacity (right). Scale bar represents 200 µm.

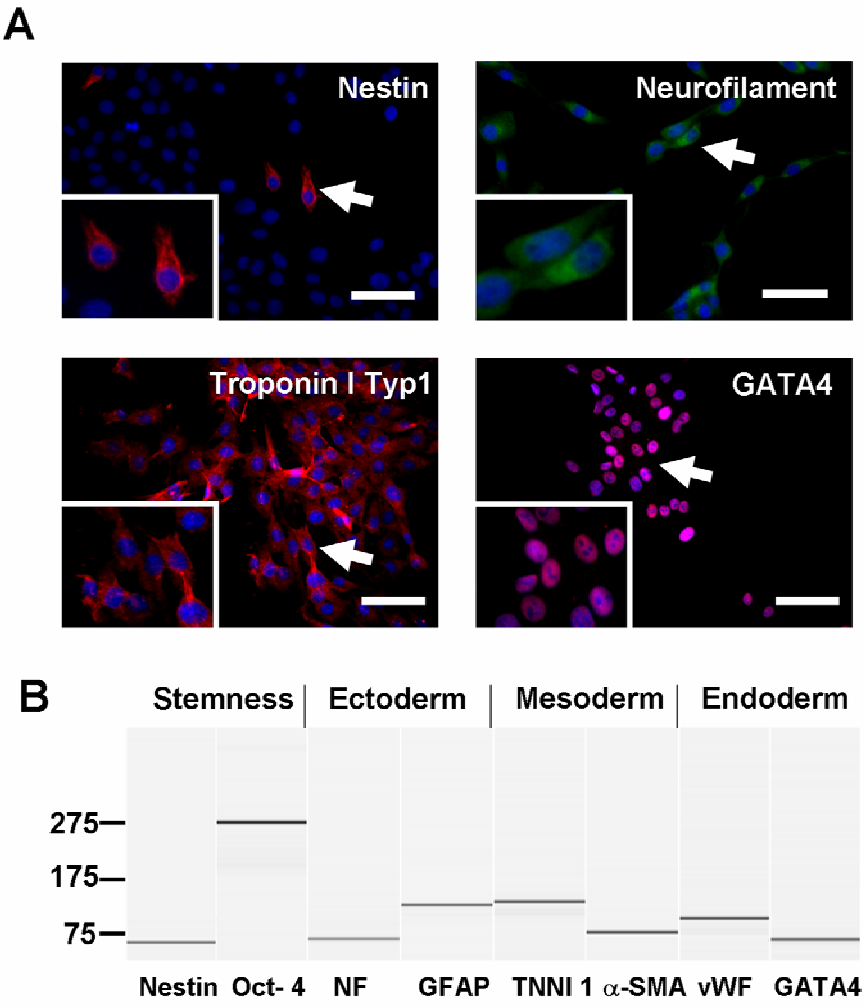

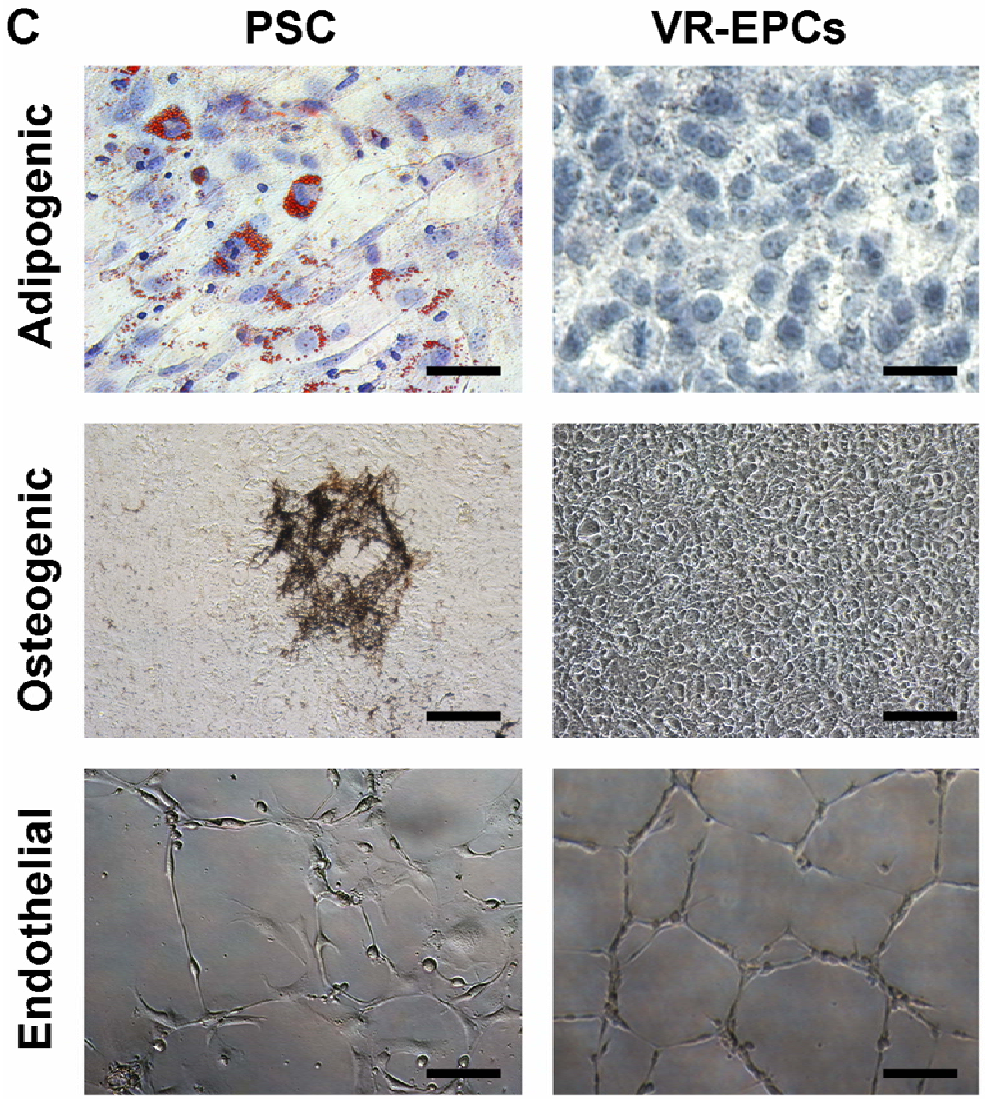

Figure 14: Differentiation potential. At protein levels (A), VR-EPCs expressed stem (Nestin) and differentiation markers (Neurofilament (NF); Troponin I type 1 (TNNI 1) and GATA4. In addition, RT-PCR analysis (B) shows that VR-EPCs express the stem cells markers Nestin and Oct-4, and differentiation markers derived from the 3 different germ layers: Ectoderm (Glial Fibrilary Acidic Protein (GFAP) and NF), Mesoderm (Alpha Smooth Muscle Actin (α-SMA) and TNNI) and Endoderm (von Willebrandt factor (vWF) and GATA4). Cell plasticity was evaluated by seeding VR-EPCs under differentiation conditions (C). In contrast to pancreatic stem cells (PSC), no formations of fat vacuoles or calcium precipitate were found after seeding VR-EPCs in adipogenic or osteogenic differentiation medium. However, well defined capillary-like structures on matrigel coated surface were observed in both, PSC and VR-EPCs. Scale bar represents 100 µm in A, 50 µm in C upper panel and 200 µm in C middle and lower panel.

5.2.2 Cell seeding in the scaffold

Next, cells were seeded in a collagen scaffold and 2 weeks later confocal

microscopic analysis was performed. A 3-dimensional reconstruction of the seeded scaffold showed that cells were distributed homogeneously, as observed by the presence of DNA staining (DAPI) in the whole structure (Figure 15A upper panel). Additional staining for actin filaments (phalloidin) showed a direct interaction between the cells and the scaffold (Figure 15A lower panel). In order to evaluate biocompatibility of the cells with scaffold, we performed MTT metabolic assays. Results showed that metabolically active cells were observed in the scaffold from day 1 (Figure 15B left panel) being metabolically active for at least 2 weeks in culture (Figure 15B right panel). A significant increase in metabolic activity was observed after 2 weeks in culture (***$p < 0.001$), suggesting cell proliferation in the scaffold.

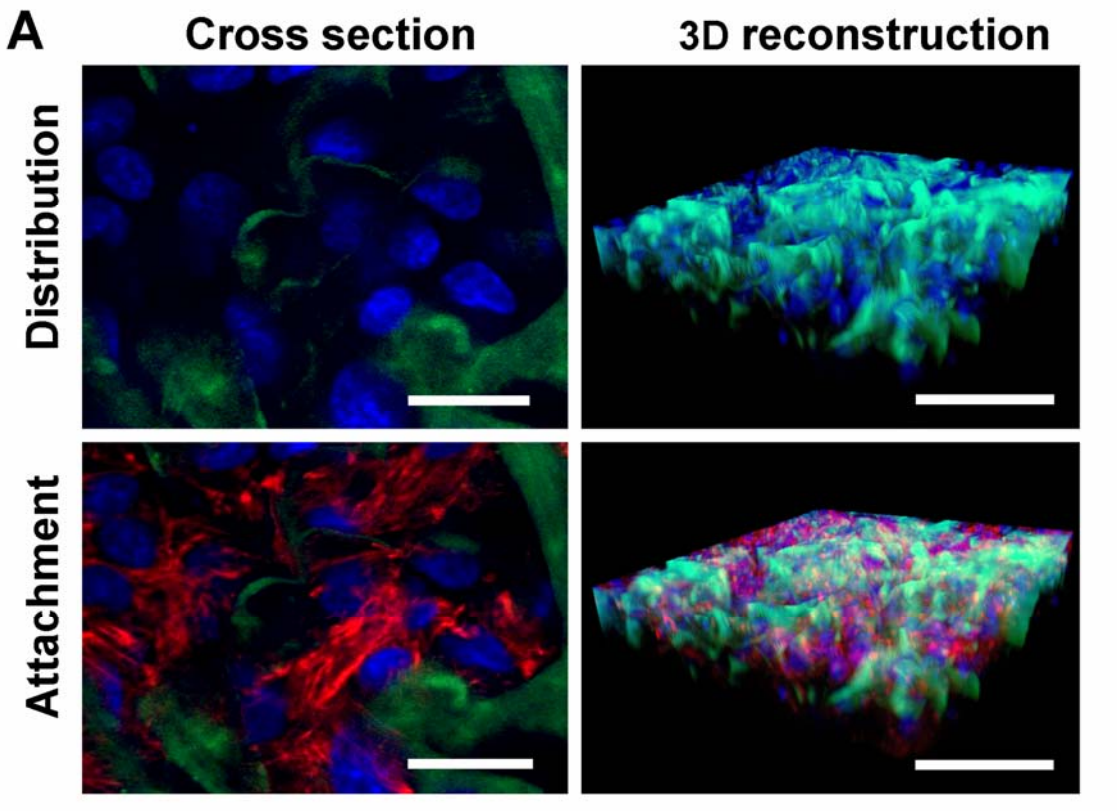

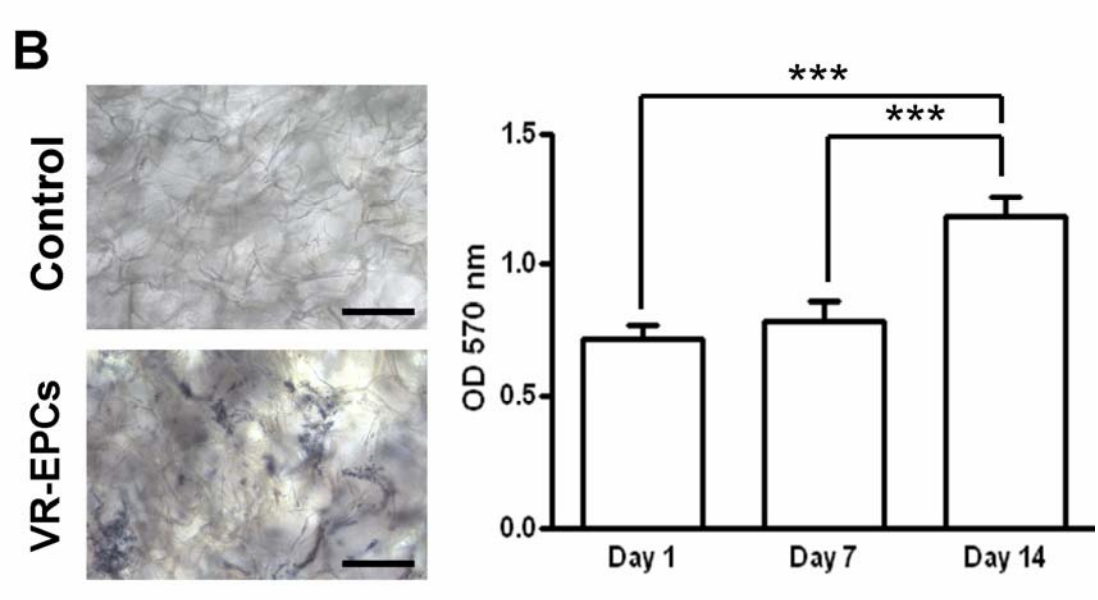

Figure 15: Cell seeding in the scaffold. Distribution (DAPI/ blue) and attachment (Phalloidin/ red) of seeded cells to the scaffold (Autofluorescence/ green) were evaluated (A). Left and panel show a representative cross section and a 3-dimentional reconstruction of the scaffold containing cells respectively. After seeding, cell viability was evaluated by MTT assays (B). Left panel shows metabolically active cells (dark blue dots) in the scaffolds. Quantification of formazan blue formation showed a significant increase in metabolic activity on day 14 after seeding. (***p<0.001). Scale bar represents 20 µm in A left panel and, 100 µm in A right panel and in B.

5.2.3 Tissue vascularization *in vivo*

In order to evaluate the capacity of the cells to increase vascularization *in vivo*, cell seeded or control (empty) scaffolds were engrafted in a bilateral full skin defect model (Figure 16). The whole procedure was well tolerated. After 2 weeks, scaffolds were removed and analyzed by tissue transillumination and digital segmentation as described before [63]. We found that the presence of VR-EPCs significantly improved vascular regeneration. Quantification of vascularization showed improvements for both vessel area and length in the seeded scaffolds (Figure 17 ***p<0.001, **p<0.01). Afterwards, vessel distribution and cellularization were evaluated by histological analyses. Results showed the presence of functional vessels in both, wound bed and scaffolds. Consistently with the results obtained by digital segmentation, a 6-fold increase

in the vessel number was observed in cell seeded scaffolds (Figure 18A *p<0.05). After, cellularization of the scaffold at the border zone was analyzed. Results showed a significant increase in cell number at the area directly over the wound bed (Figure 18B *p<0.05).

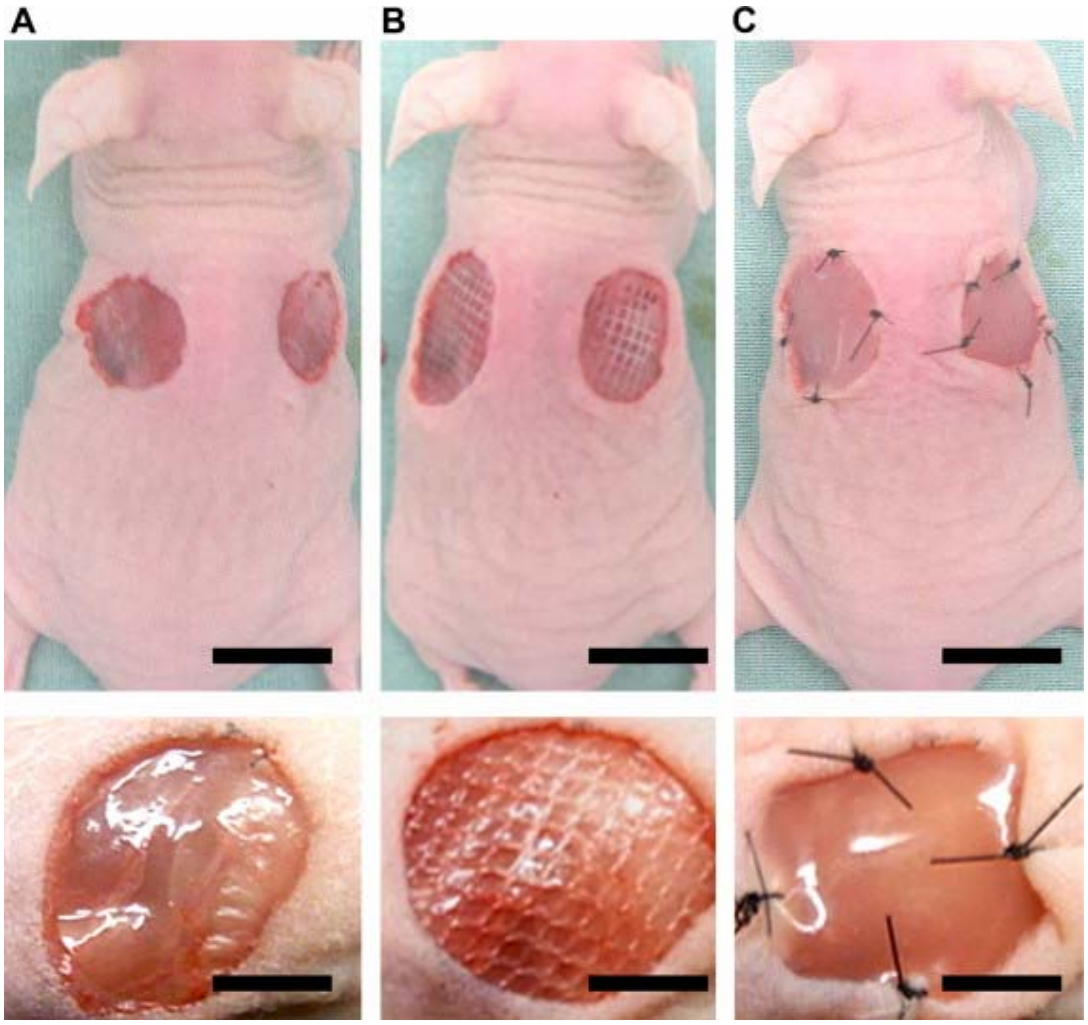

Figure 16: Full skin dermal regeneration mouse model. 10 mm diameter bilateral defect was created in the back of the animal (A). In order to minimize possible artifacts during the tissue harvesting, a titanized mesh was placed between the wound bed and the scaffold (B). Finally, the wound was covered with a scaffold for dermal regeneration (C). Scale bar represents 1 cm in the upper row and 0.5 cm in the lower.

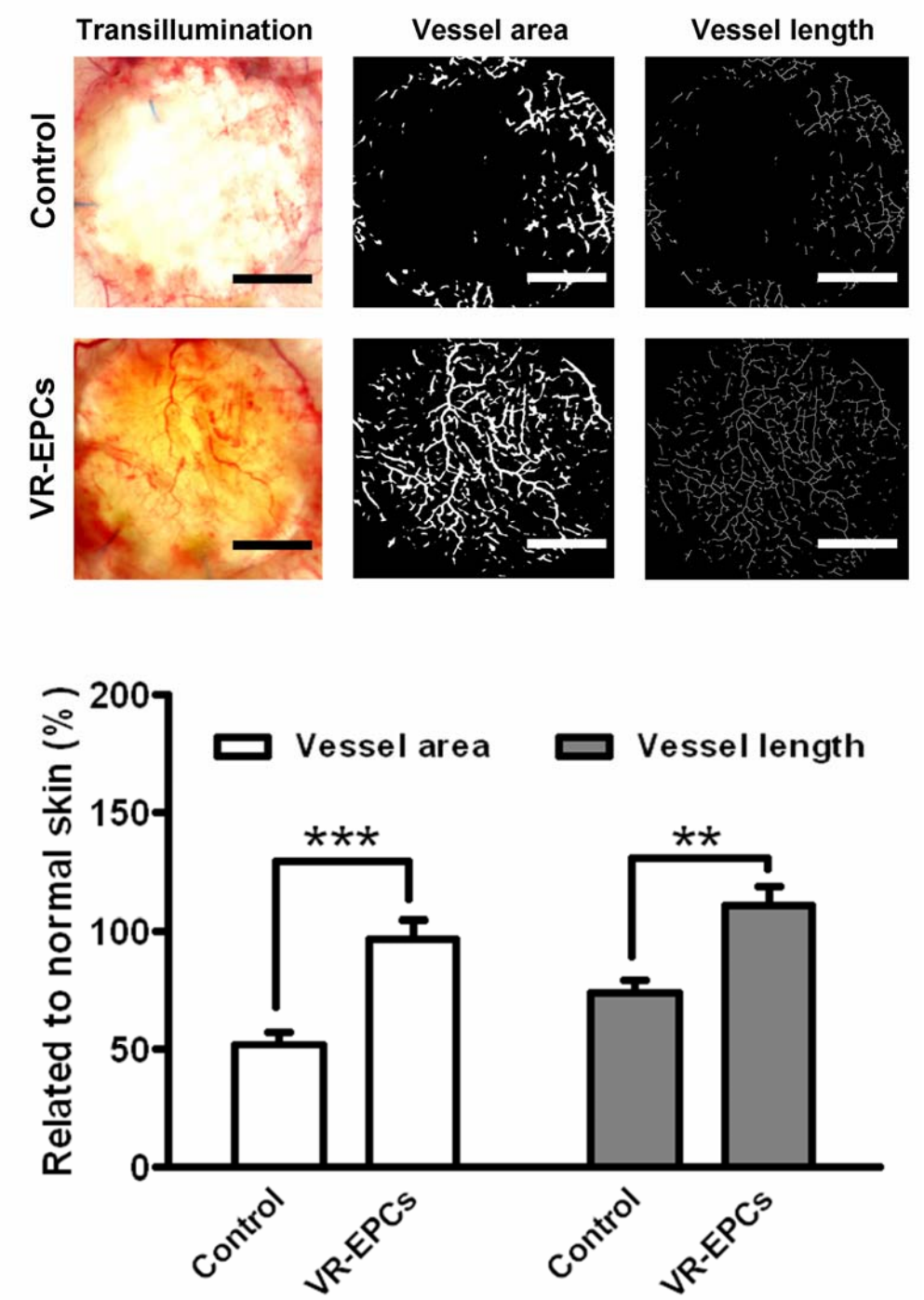

Figure 17: Vascularization of the scaffold *in vivo*. Neovascularization of the scaffold was analyzed 2 weeks after transplantation. A representative scaffold of each group is shown by transillumination and digital segmentation (vessel area and vessel length). Quantification of the digital segmentation showed that seeded scaffolds (VR-EPCs; n=10) were significantly more vascularized than controls (empty scaffolds; n=8) in both, vessel area (*** $p<0.001$) and vessel length (** $p<0.01$). Scale bar represents 3 mm.

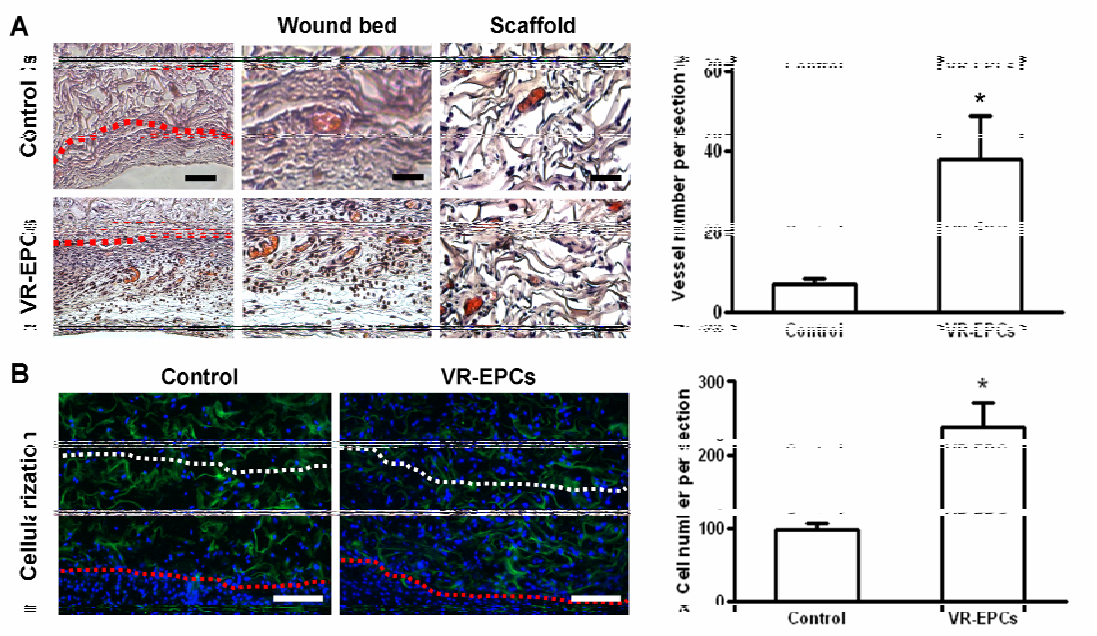

Figure 18: Histological analysis. Sections of the scaffold showed that functional blood vessels were distributed in both, wound bed and scaffold, which are observed under and over the red dot line (A). Quantification of the number of blood vessels per section shows that the presence of VR-EPCs increased the vascularization levels (* $p<0.05$). Cellularization of the scaffolds was quantified by counting the number of cells present at the border zone (between the red and white dot line). Results showed that in seeded scaffolds the number of cells was increased when compared to controls (B; *$p<0.05$). Scale bar represents 200 μm in A (left panel) and B and, 50 μm in central and right panels in A.

5.2.4 Cell behavior under pro-angiogenic conditions

In order to determine the possible mechanisms involved in the vascular regeneration *in vivo* by VR-EPCs, here we analyzed cells under proangiogenic environments. After seeding cells on polystyrene surface, the presence of endothelial growth medium (EGM) induced the formation of capillary like structures (Figure 19A). The number of such structures was also found to be increased when cells were cultured on matrigel coated surfaces (Figure 19B; *$p < 0.05$). In addition, cells responded to EGM by increasing their migration capacity evaluated by a scratch assay (Figure 19D; ***$p < 0.001$). Interestingly, MTT assays showed that the presence of angiogenic factors decreased the metabolic activity of the cells (Figure 19C *$p<0.05$).

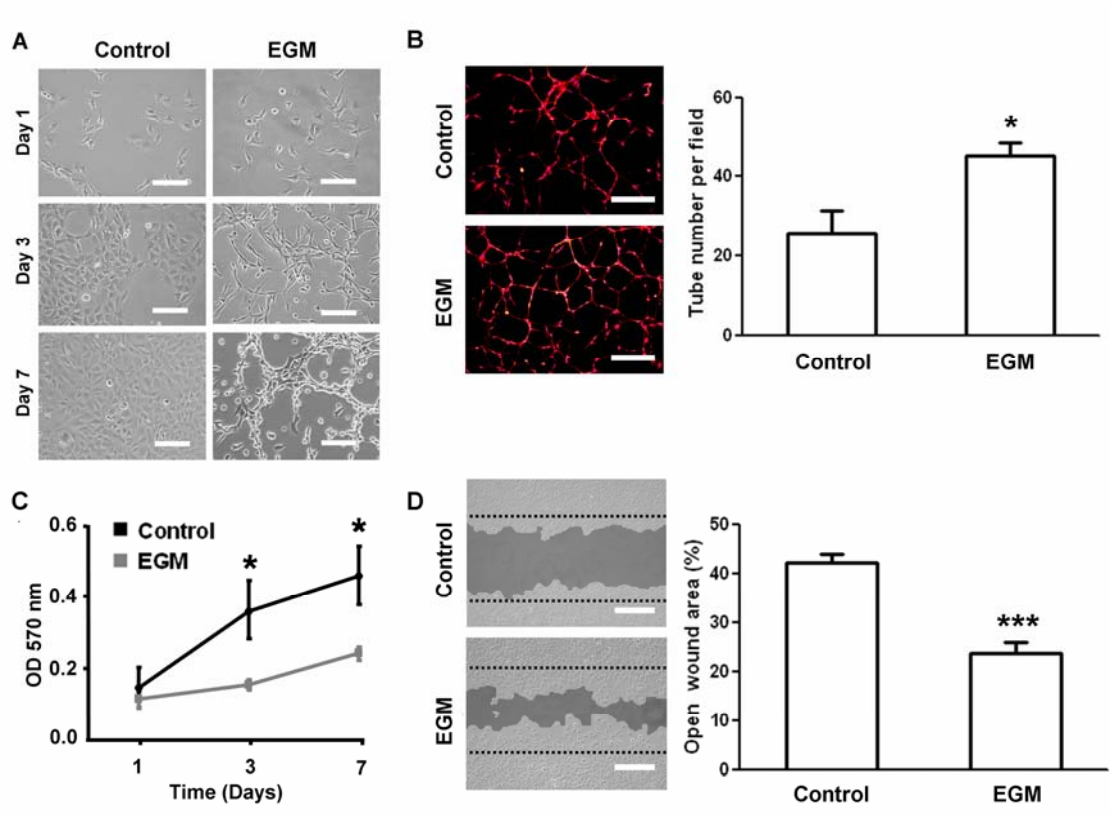

Figure 19: Behavior of VR-EPCs in pro-angiogenic environments. Cells were cultured in control (DMEM + 10% FCS) or pro-angiogenic environments (Endothelial Growth Medium/ EGM) and their behavior was compared. A dramatic change in morphology was observed when cultured in EGM (A). Moreover, EGM enhanced the ability of the cells to form capillary-like structures on matrigel coated surfaces (B), decrease metabolic activity (C) and, increased cell migration rate in a scratch assay (D). Scale bar represents 100 µm in A and, 200 µm in B and C. (*p<0.05; ***p<0.001).

5.2.5 Paracrine profile of VR-EPCs

It has been proven that stem/progenitor cells might contribute to neovascularization by releasing different soluble growth factors [70]. In order to determine whether VR-EPC can also contribute in this manner, we performed a cytokine antibody array. Here we have found that conditioned media contains chemoattractant (CXCL-1, MCP-1), and angiogenic (VEGF and PDGF-AA) molecules. Moreover, proteins related to tissue remodeling (TIMP-1, Activin A and Agrin) were also detected (Figure 20).

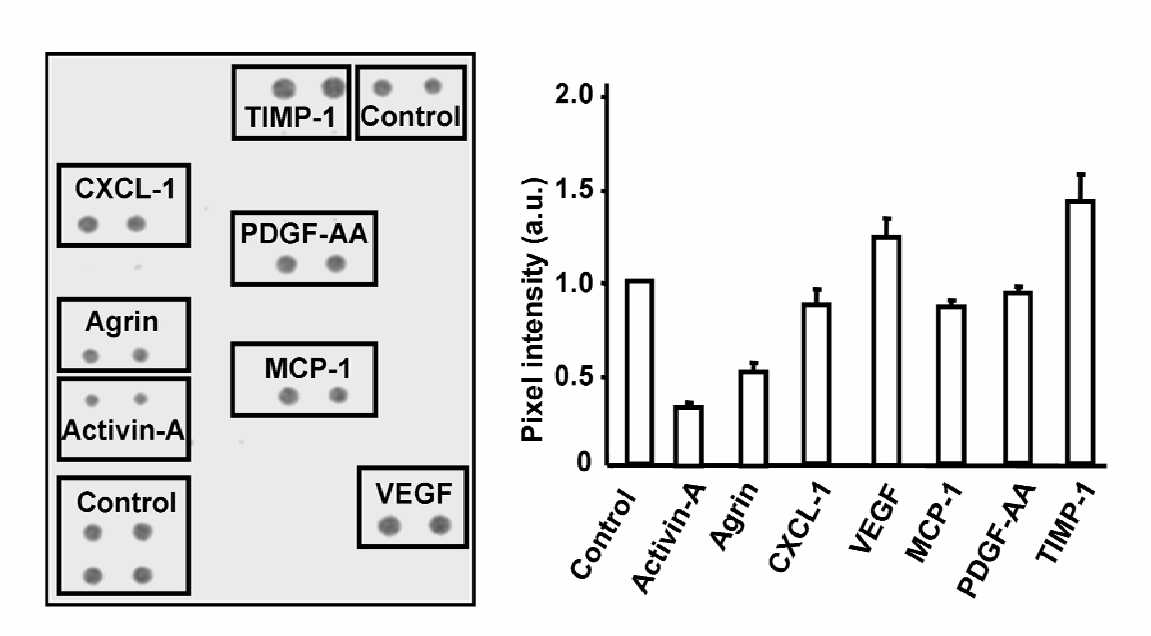

Figure 20: Paracrine profile of VR-EPCs. The release of bioactive molecules from VR-EPCs was evaluated by cytokine protein array. After 3 days in culture, several bioactive molecules were found in the conditioned medium including: Agrin, Activin-A, CXCL-1, PDGF-AA, MCP-1, TIMP-1 and VEGF. Relative secretion was evaluated as pixel intensity related to the positive control.

5.3 Results from objective 3

5.3.1 Isolation and characterization of primary dermal fibroblasts

Isolated rat dermal fibroblasts were spindle-shaped and adhered rapidly to the culture flasks (Figure 21A). The characteristics of these primary fibroblasts were detected by cytospin for the expression of prolyl 4-hydroxylase subunit beta (P4H beta). A fluorescent microscopic imaging for the expression of P4H beta is presented (Figure 21B). In addition, the actin cytoskeleton morphology of the fixed and permeabilized cells was also examined by FITC-label phalloidin under sub-confluent and confluent conditions (Figure 21 C and D), which indicated the nature of smooth muscle cells. The cell growth curve was obtained with normal culture medium (DMEM+10%FCS), showing an active cell replication with a doubling time of 24–48 hours. Cell growth was linear during the first 7 days and then reached a plateau phase on day 8 (Figure

21E).

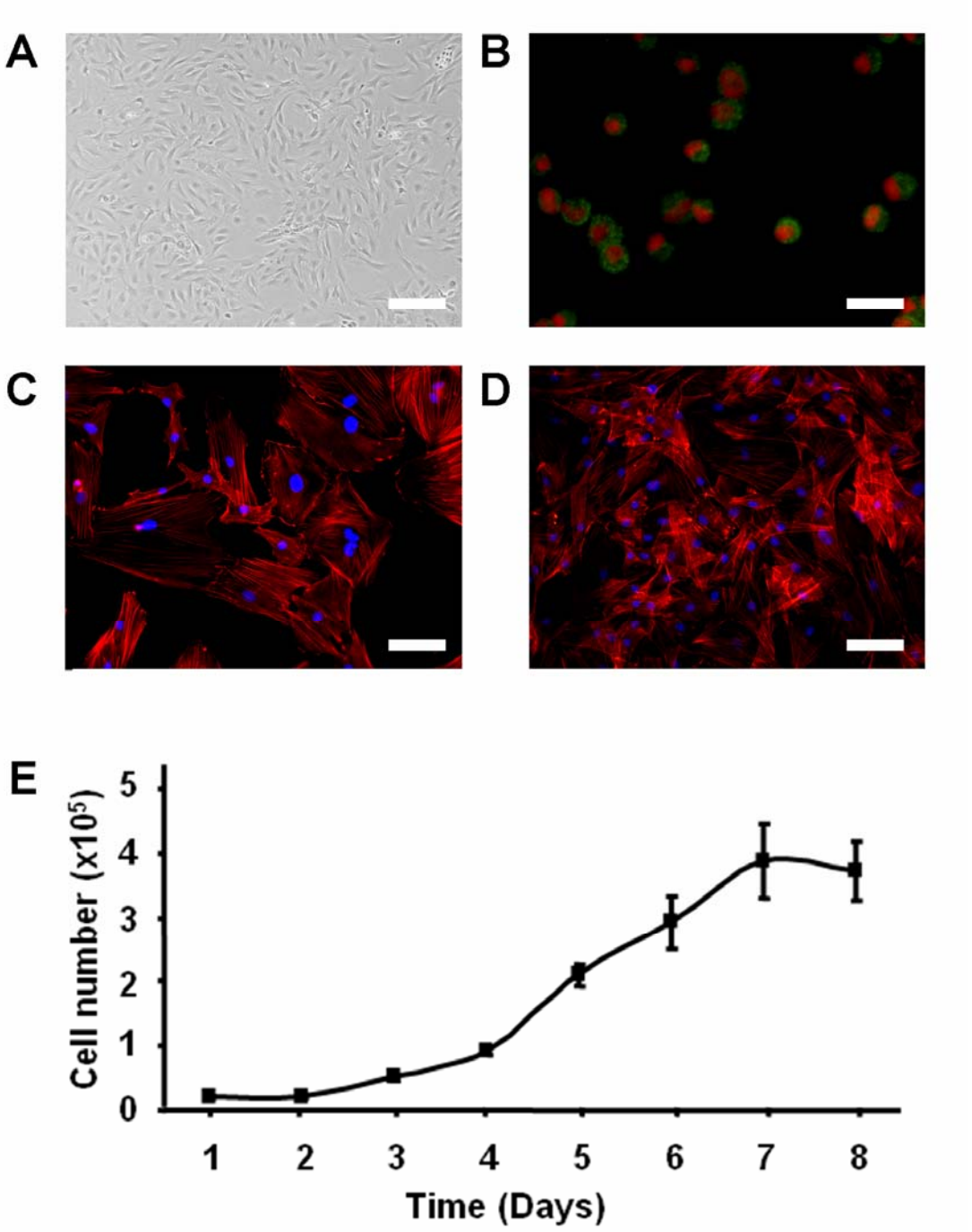

Figure 21: Preparation and characterization of rat primary fibroblasts. (A) Morphology of rat dermal primary fibroblasts (passage 2) was shown under phase contract microscope. (B) Characterization of isolated fibroblast with anit-fibroblast antibody (Prolyl 4-hydroxylase subunit beta: P4H beta), green: P4Hbeta; red: PI nucleus staining. (C) Morphology of fibroblasts under subconfluent and (D) confluent conditions was analyzed by phalloidin (red) and DAPI (blue) staining. (E) Primary rat dermal fibroblasts (passage 2) growth curve. Scale bar represents 200 µm in A, 100 µm in B and D, 50 µm in C.

5.3.2 Optimization of nucleofection with improved reagents

We first examined transfection efficiency with six nucleofector programs (including A24, T16, U12, U23, U30, and V13). The cells were transfected with commercial protocol provided by the manufacturer. The highest transfection efficiency (around 60%) and cell viability (>95%) were obtained with program U30. Therefore, program U30 was chosen for further *in vitro* and *in vivo* experiments.

To achieve the maximal therapeutic effects, nucleofection reagents were modified to improve gene transfection efficiency in primary cell cultures of fibroblasts (details described in Materials and Methods). Two days after nucleofection, the total number of cells significantly decreased in the control group, in which commercial kit reagents were used (Figure 22A, upper panels). When transfected reagents were modified, transfection efficiency, as shown by more GFP-positive cells, was enhanced (Figure 22A, lower panels). With such improved reagents, 2 days after nucleofection, more transfected cells were obtained in contrast to the control standard protocol (Figure 22B, left panel: 0.42 ± 0.35 (Improved) vs. 1.07 ± 0.29 (Control); *$p<0.05$). By FACS, we found that the use of modified solution did not affect cell growth, but induced higher transfection rate (Figure 22B, right panel: 80. 5 ± 5.0 (Improved) vs. 51.5±7.9 (Control); **$p<0.01$).

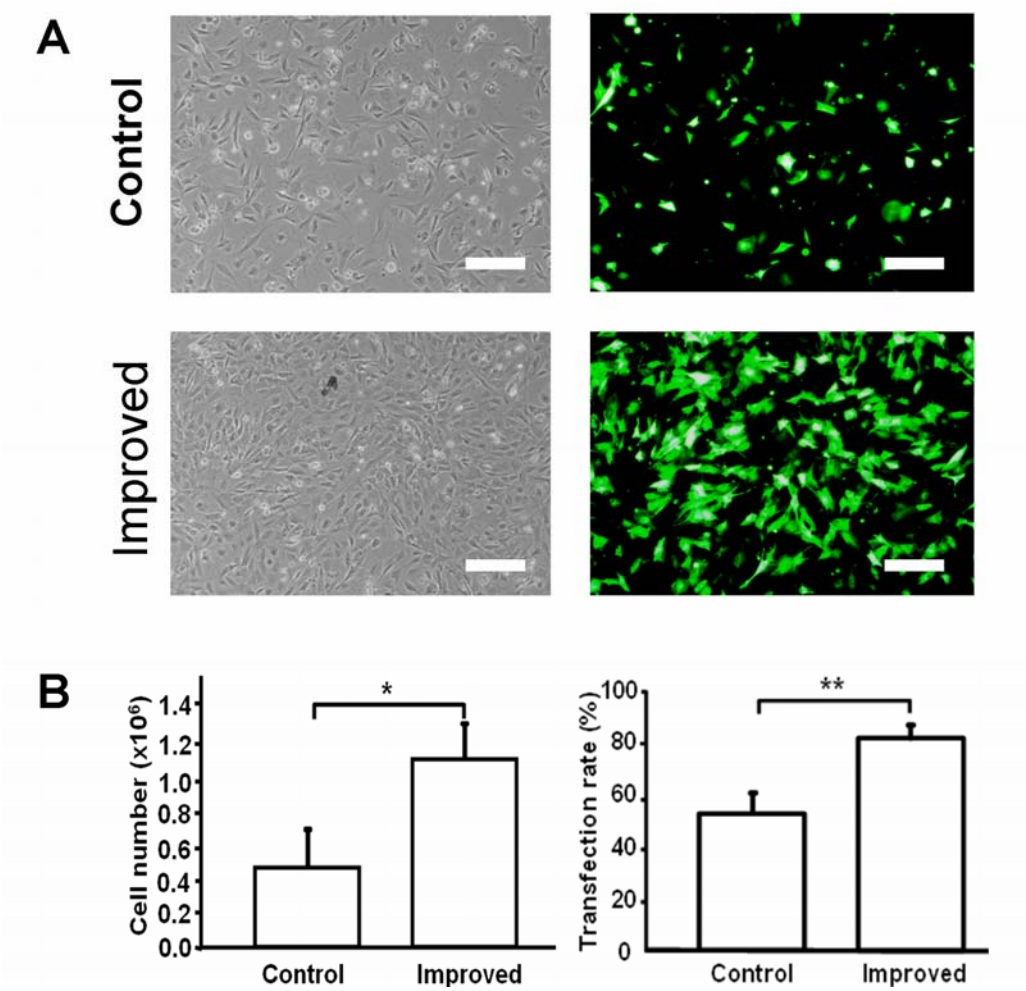

Figure 22: Optimization of nucleofection in primary cultures of fibroblasts. (A) Improved method (improved) and original method (control) were compared under fluorescence microscope to show optimization of nucleofection. Representative pictures of each method are shown in this panel. Scale bar represents 100 μm. (B) Cell number and transfection rate were significantly enhanced by the improved method (experiment was repeated for more than 5 times; * $p<0.05$; ** $p<0.01$).

5.3.3 Dermal fibroblast nucleofection with VEGF and bFGF plasmid

After optimization with pmaxGFP vector, VEGF165 and bFGF sequences were inserted into the pmaxGFP® backbone as coding sequences. Seven days later, significantly more cells were observed in the group transfected with plasmids expressing bFGF when compared with the control (Figure 23A). Next, the growth-factor release was evaluated daily for 21 days (Figure 23B). Long-term expressions of both VEGF165 and bFGF proteins were found after

nucleofection, and the dynamics of their release were similar. Both growth factors reached the expression or release peak at the first week. However, the amount of secreted growth factors was different between both the groups, with about 50-fold higher release of VEGF165 than bFGF.

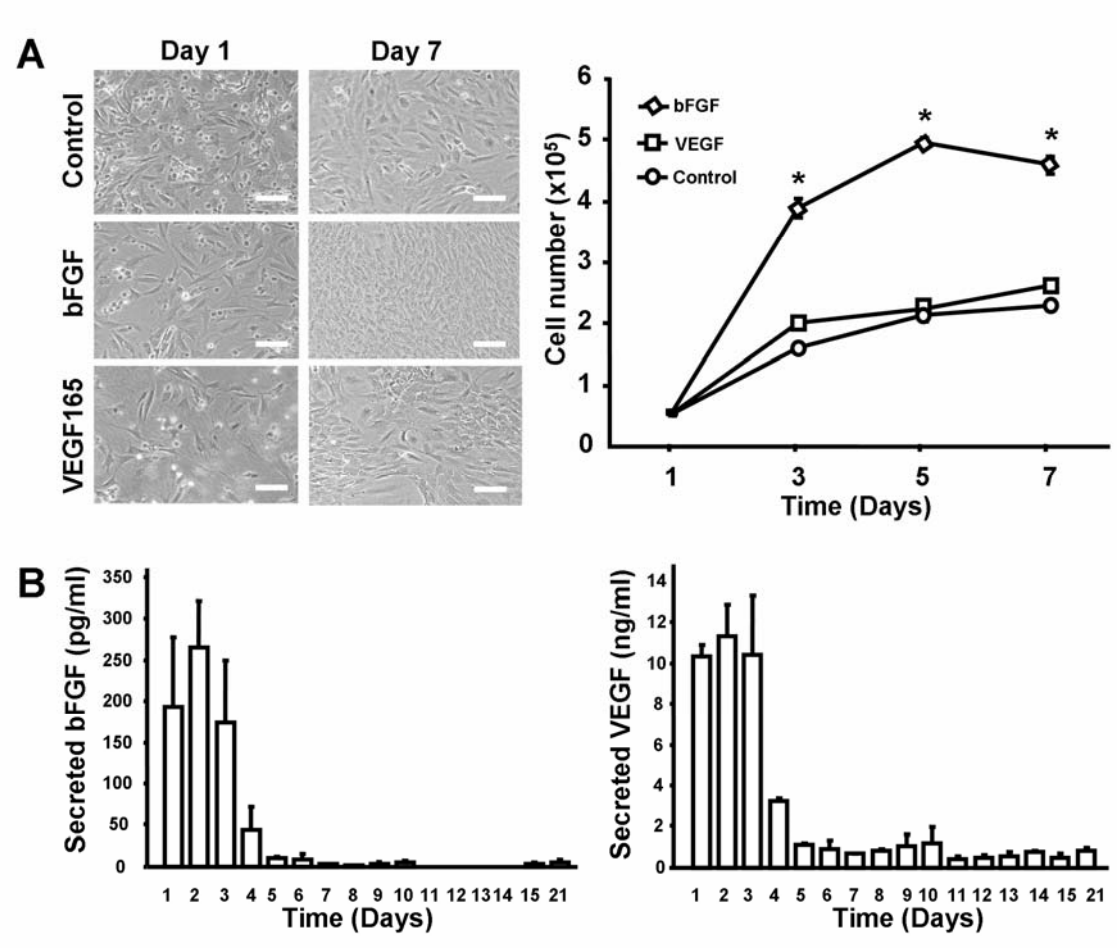

Figure 23: Cell growth and gene expression in primary cultures of fibroblasts transfected with bFGF and VEGF plasmids. After Nucleofection, 1.4 x 10^5 cells were seeded in a 12 wells plate, 1.5 ml of the culture medium was changed every day. (A) 7 days after Nucleofection, more cells were observed in transfected groups. Quantification showed that significant differences were found between bFGF nucleofected group and control group (* $p<0.05$). (B) Recombinant growth factors were detected for up to 21 days in the culture media. Scale bar represents 100 µm.

5.3.4 *In vivo* gene-delivery efficiency by nucleofected primary dermal fibroblasts

After administration of genetically modified fibroblasts, distribution of the

plasmids in the peripheral tissues or organs was detected by real-time PCR. No plasmid could be detected in any organs of the control rats injected with nonmodified cells. The plasmid was detected for more than 28 days at the site of injection (Figure 24A). The peak of expression at the injection site was on day 3, and then remained at a fairly high level. From day 3 to day 7, the plasmid concentration dropped rapidly. After day 7, the local concentration was maintained at the level of 105 copies/100 ng DNA, and then deceased to the order of 103 copies/100 ng DNA on day 28. Expression of bFGF and VEGF165 was also detected by PCR at the site of injection. On day 7 post injection, the expression of both angiogenic growth factors in the muscles was more than 100-folds higher than that in the control group (Figure 24B). In all peripheral tissues and organs from the experimental rats, no plasmid was detected after day 14 (Figure 24C).

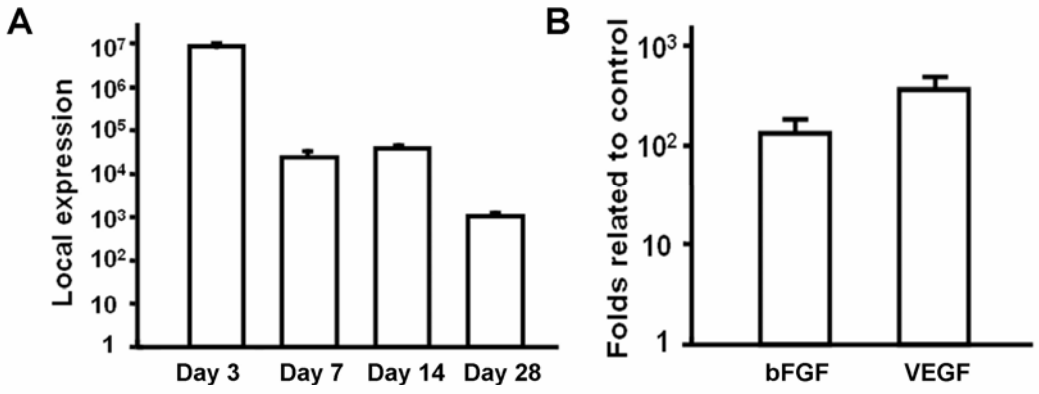

C

Tissue	Day 3	Day 7	Day 14	Day 28
Testis	5.8 ± 0.2	9.6 ± 0.1	N	N
Kidney	6.6 ± 3.4	9.6 ± 5.3	N	N
Heart	86.9 ±34.5	N	N	N
Spleen	10.3 ± 7.8	117.5 ± 56.2	N	N
Liver	1.9 ±3.2	N	N	N

Figure 24: Gene delivery efficiency and expression *in vivo* by modified primary dermal fibroblasts. (A) High levels of plasmids were detected in the injected area for more than 28 days. (B) 7 days after cell injection, gene expressions of bFGF and VEGF165 from injected area were measured. Results showed that the expressions of both bFGF and VEGF165 were 100 times increased related to the control group. (C) After cell administration, organs or tissues were collected at 4 different time points (experimental group: n=3; control group: n=3) and the sequence of the plasmid backbone was used for detection of its distribution. Results are shown as the average value obtained from 100 ng DNA of each organ or tissue. N represents that no plasmids were detected.

5.3.5 Administration of nucleofected fibroblasts enhanced angiogenesis and arteriogenesis in the ischemic zone

After cell administration, the ischemic zone was reconstructed (Figure 25A) and the collateral was counted in 3D reconstruction views (Figure 25B). A significant increase in the number of vessels was triggered by the injection of nucleofected cells (Figure 26A and B; *$p<0.05$). Quantification was conducted after reconstruction of the ischemic zone (Figure 27A). Both angiogenesis (Figure 27B, right upper panel; 3.61 ± 0.56 vs. 5.13 ± 1.08 *$p<0.05$) and arteriogenesis (Figure 27B, right lower panel; 1.33 ± 0.09 vs. 1.63 ± 0.06, *$p<0.05$) increased, indicating an improvement in the medium-size vessel and related small and thin vascular networks.

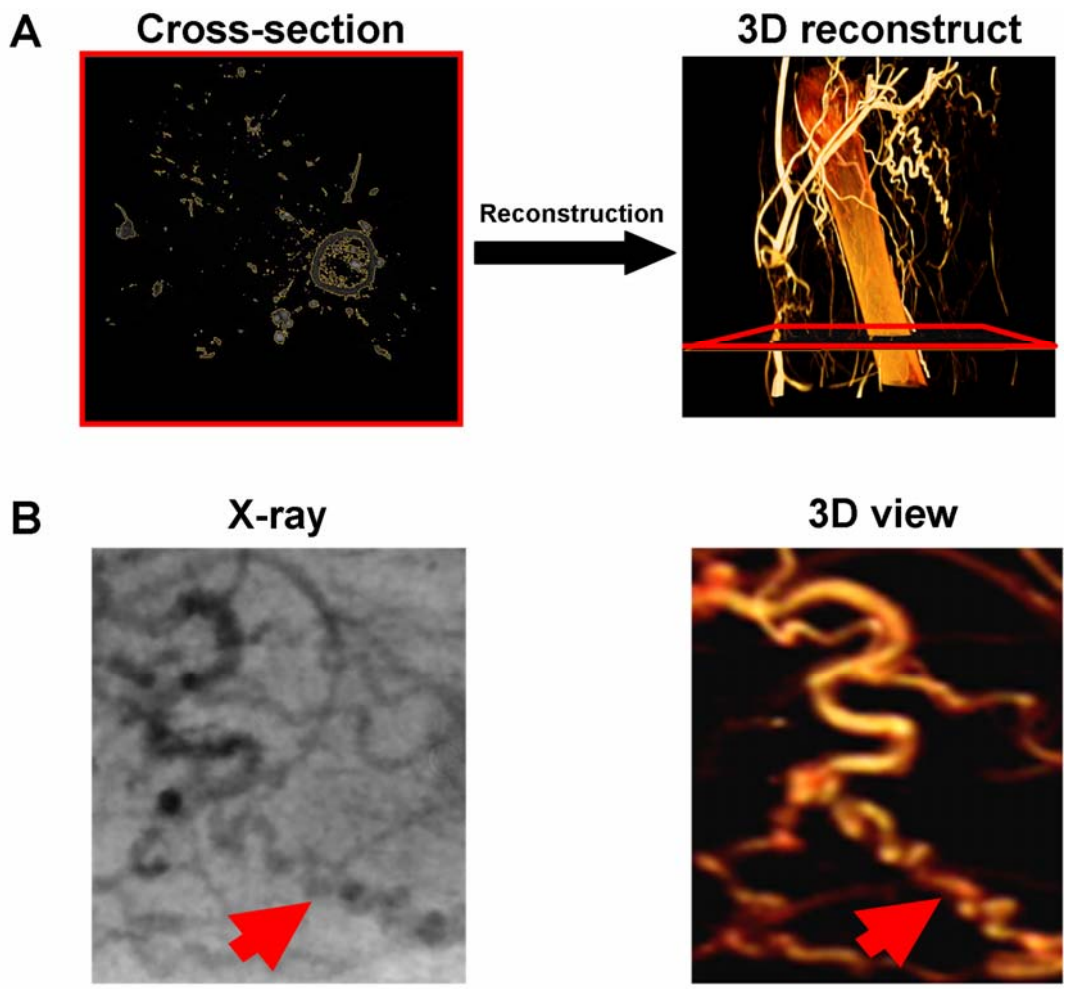

Figure 25: Comparison of micro-CT 3 dimensional collateral detection with planar method. (A) Ischemic hindlimb was reconstructed through 1024 Z-axis slices (left panel). (B) Vessels in 3 dimensional (3D) reconstruction views were analyzed. Red arrows show the same corkscrew collateral vessel in both X-ray review and 3D reconstruction view.

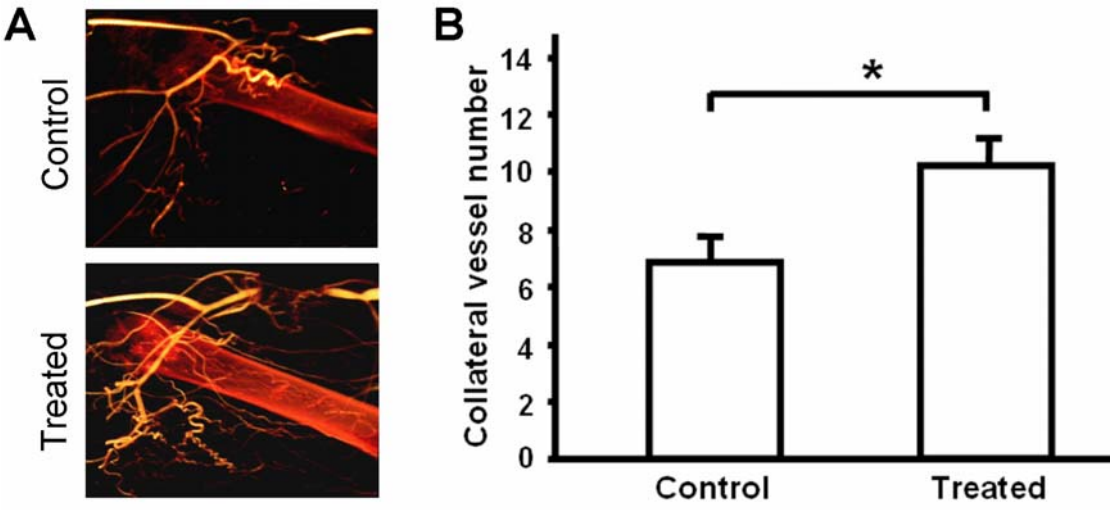

Figure 26: Increased 3D collateral vessels in ischemic hindlimbs treated with nucleofected fibroblasts. (A) One week after cell administration, micro-CT angiography was performed and the ischemic zone from both treated and control samples were reconstructed. (B) Summarized data showed that injection of transfected cells increased the number of visible collateral vessels (treated group: n=7; control group: n=6 *p<0.05).

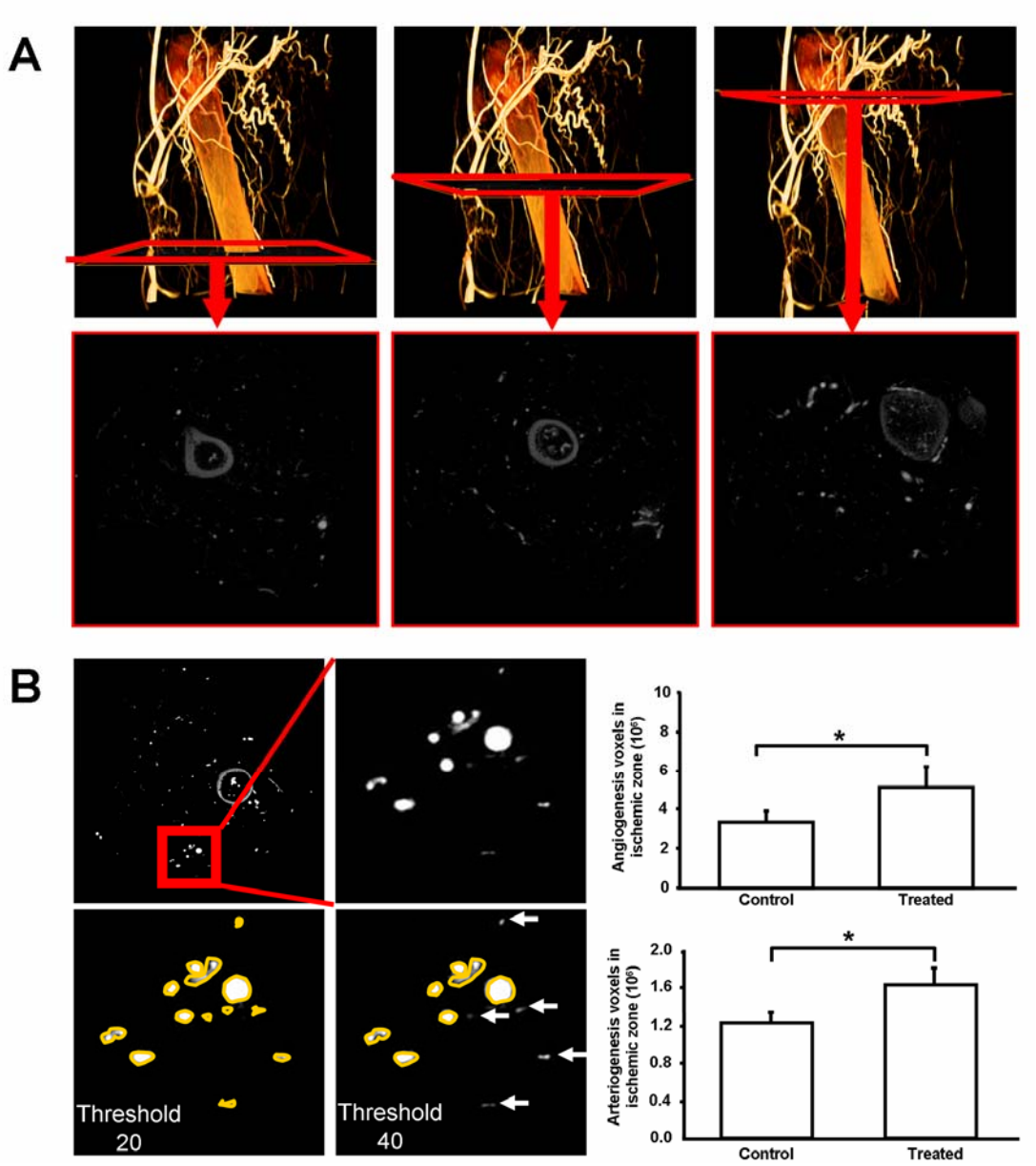

Figure 27: Increased vascular volume in ischemic hindlimbs treated with nucleofected fibroblasts. (A) The ischemic zone was defined as 600 slices below the proximal ligation point (slices from the left panel to right panel), including the distal ligation point in the middle panel. (B) Quantification was done with 2 different thresholds: T20 and T40. With threshold 20, all vessels (angiogenesis and arteriogenesis related) were counted. Threshold 40 was used to quantify only vessels with higher caliber (arteriogenesis related). (C and D) Vessels related to angiogenesis and arteriogenesis were significantly enhanced after nucleofected fibroblasts injection (treated group: n=7; control group: n=6; Angiogenesis: * p<0.05, Arteriogenesis: *p<0.05).

5.3.6 Increased collateral growth and blood flow in ischemic hindlimbs treated with nucleofected fibroblasts

To further examine the effects of nucleofected cells on collateral growth, collateral proliferation index was analyzed after local administration of nucleofected cells. The results showed an enhanced collateral proliferation in the same model (Figure 28A, BrdU incorporation: 0.48 ± 0.05 vs. 0.57 ± 0.05; *p<0.05). Re-establishment of a collateral circulation in ischemic lower hindlimbs was detected by fluorescent microspheres. These microspheres were trapped inside the lumen of the small arteries and the number of the microspheres inside each muscle is related to the blood flow (Figure 28B, left panel). Microspheres from both soleus and gastrocnemius (ligated and nonligated hindlimbs) were counted under fluorescent microscope to obtain the perfusion ratio from each animal. Blood flow from soleus and gastrocnemius significantly increased after administration of nucleofected cells (Figure 28B, right; microspheres ratio: gastrocnemius: 0.41±0.10 vs. 0.50±0.11; *p<0.05; soleus ratio: soleus: 0.42±0.08 vs. 0.60±0.08; **p<0.01).

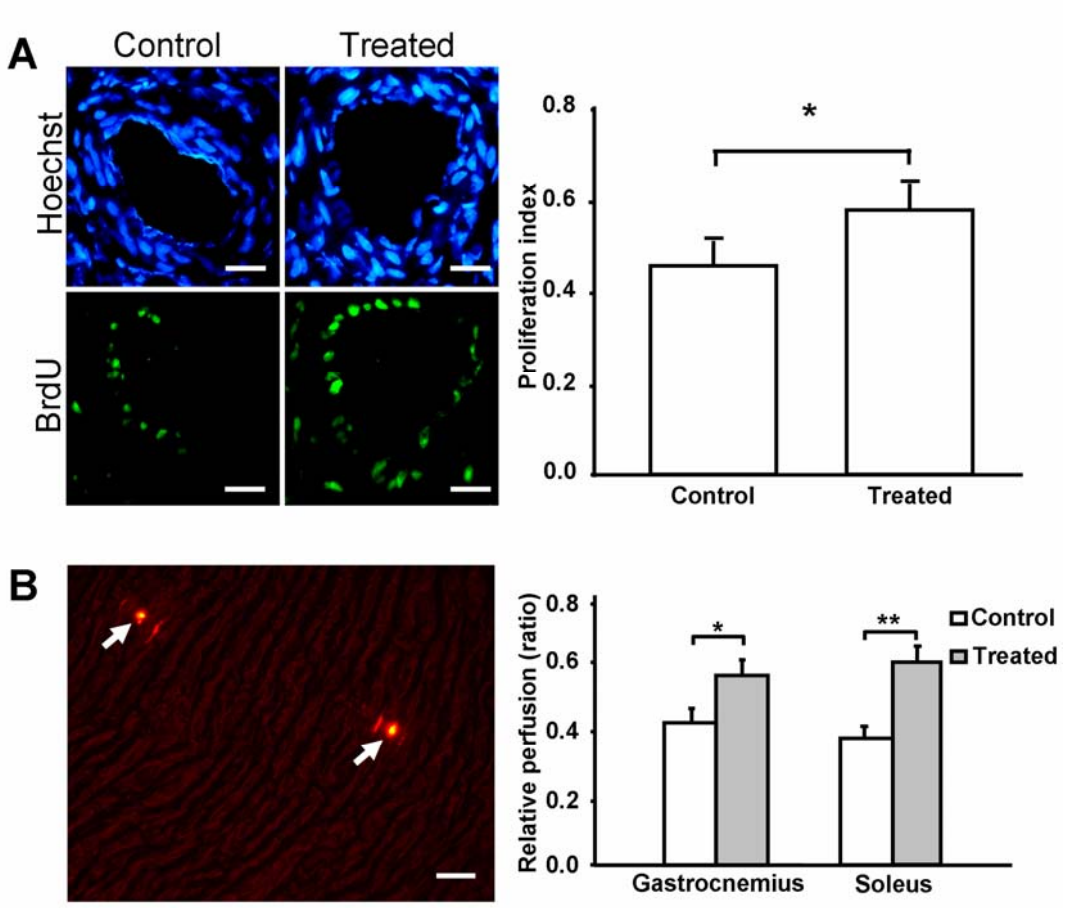

Figure 28: Increased collateral growth and blood flow in ischemic hindlimbs treated with nucleofected fibroblasts. (A) One week after cell administration, collateral growth was detected and quantified by BrdU and Hoechst staining. The proliferation index is expressed as BrdU (green) positive nuclei *vs*. total (Hoechst/ blue). Quantification showed that proliferation index was significantly enhanced by the injection of transfected cells (Experimental group: n=8; control group: n=7,* $p<0.05$). Scale bar represents 50 µm. (B) Blood flow was analyzed by FluoSpheres® blood flow detection method. Cryosections were analyzed by fluorescent microscopy and the numbers of the microspheres per muscle sample were counted (left panel). The white arrows show the fluorescent microspheres trapped in the small capillaries. Blood flow ratio was calculated as numbers of microspheres trapped in the ligated muscle *vs.* the number trapped in the same part of the non-ligated leg in the same animal. Results are shown as gastrocnemius perfusion ratio between control and experimental group; soleus perfusion ratio between control group and experimental group (right panel). In both muscles, the blood flow was significantly improved (Experimental group: n=8; control group: n=7 soleus: **$p<0.01$ gastrocnemius *$p<0.05$). Scale bar represents 50 µm.

6. DISCUSSION

Previous evidence had shown that keratinocytes and fibroblasts can be cultured in Integra matrix *in vitro* [71]. Similarly, our results from objective 1 show that human sweat gland-derived stem cells (SGSC) can also be seeded in collagen scaffolds (Figure 10), thus representing a novel and promising cell source for activating scaffolds for tissue regeneration. In the present work we show that SGSC are easy to isolate, giving rise to an adherent cell population that can be robustly expanded *ex vivo* (Figure 8b), allowing obtaining therapeutic numbers of autologous cells in clinical time frames. We have previously described similar properties for stem cells derived from other exocrine glands such as pancreas and salivary glands [31]. However the easy accessibility and low collateral damage associated to the harvesting of sweat glands represents a big advantage when compared to other exocrine glands. In case of allogenic transplantations of SGSC their immunogenicity have to be evaluated and compared to other well described stem cells populations. For instance, several reports have shown successful results by using allogenic mesenchymal stem cells in different clinical settings [72, 73].

In the present study, we have demonstrated that SGSC improve vascularization during scaffold-dependent dermal regeneration *in vivo* (Figure 12a). Here we have shown that SGSC responded to pro-angiogenic environments, increasing their proliferation and migration capacity and forming capillary-like structures (Figure 9). Additionally, we have found that SGSC express the endothelial markers von Willebrand factor and alpha smooth muscle actin (Figure 8). These data support the hypothesis that SGSC may

improve tissue regeneration by direct differentiation into vessel-related cells (e.g. endothelial cells). As an alternative mechanism of contribution, SGSC may also act as trophic mediators, rather than by direct cell differentiation, thus helping to create a pro-regenerative microenvironment in the wound area. This concept has been clearly established before for other stem cell such as mesenchymal stem cells, which may contribute to tissue regeneration by releasing chemotactic, immunomodulatory and pro-angiogenic factors [74]. We have previously shown that the release of angiogenic factors from cell seeded scaffolds might enhance angiogenesis independently of cell differentiation [31]. Here we show that, in contrast to control scaffolds (data not shown), SGSC seeded scaffolds release at least 11 bioactive molecules (Figure 10c). Among them, Angiogenin and VEGF are particularly important because it has been described that both molecules have a direct effect on angiogenesis [75]. The release of the chemokine IL-8 and the factor Pentraxin 3 (PTX3) suggest that SGSC might also play an immunomodulatory role during tissue regeneration. Finally, the release of the metalloproteinase MMP-9 and the metalloproteinase inhibitor TIMP-1 might play a role later on in the process of tissue remodeling [76]. Those results and the high biocompatibility observed between SGSC and Integra matrix suggests that SGSC-seeded scaffolds may represent a constant source for releasing bioactive molecules during wound healing *in vivo* (Figure. 10).

Unexpectedly, in this work we have also found that the presence of SGSC decreased the cellularization levels of the scaffold, while the thickness of the wound bed directly below the Integra matrix increased. Here we hypothesize

that such decrease in cellularization is due to a paracrine anti-inflammatory effect of the seeded SGSC which inhibit the migration of mononuclear cells into the scaffold. Instead, tissue remodeling and revascularization is triggered by the seeded cells, thus increasing the wound bed thickness. Since this reasoning is very speculative, a better understanding of the mechanisms in SGSC-assisted wound healing is required. Among others, a general characterization of the cell types observed in the wound area and their state of proliferation and migration should be studied in more detail.

Although our results support the idea that SGSC might contribute to vascularization by direct differentiation and trophic mediation, further studies have to be performed to better understand their mechanisms of contribution. Among others, the full spectrum of molecules released from seeded scaffolds and their impact on angiogenesis have to be determined *in vivo*. In addition, co-localization of the engrafted cells with the newly formed vascular network in the scaffold is required to determine the contribution of SGSC to vasculogenesis. The possibility of using SGSC combined with different biomaterials or cell carriers is another issue that should be addressed in future research. Finally, further studies should also be addressed to evaluate the physiological meaning of the presence of such stem cells in sweat glands and their regenerative potential in their own niche.

The results from objective 2 have demonstrated that highly clonogenic vascular resident endothelial progenitor cells (VR-EPCs) could be used to induce postnatal neovascularization in tissue engineering and regeneration.

VR-EPCs showed several stem/progenitor cells features (Figure 14) *in vitro* and might contribute in direct (Figure 19) and/or paracrine manners (Figure 20) to vascularization *in vivo* in a scaffold based nude mice full skin defect model (Figure 16, 17 and 18).

Nowadays, there is a broad consensus that for most tissues and organs, vascularization is the key process for regeneration. Thus, autologous endothelial progenitor cells represent an attractive target cell source for therapeutic neovascularization. Since the discovery of endothelial progenitors in 1997, the definition and exact location of such cells have been under debate [38]. The current study presented 3 lines of evidences showing that our cells might represent a new type of EPCs. First, VR-EPCs obtained from a single cell clone have showed a highly clonogenic ability with a doubling time of approximately 18 hours (Figure 13). Although VR-EPCs were isolated from a single cell clone, they showed differentiation markers expressed in cells derived from all 3 different germ layers (Figure 14 A and B). Moreover, we also found nestin positive stem cell clones from the late outgrowth population (Figure. 14A). Second, compared to cells cultured under control condition (DMEM + 10% FCS), VR-EPCs cultured in endothelial cell growth medium showed a different phenotype (Figure 19) including the formation of capillary like structures on polystyrene and matrigel surface and the enhancement of cell migration ability. Furthermore, when seeded in scaffolds for *in vivo* dermal regeneration, VR-EPCs showed significant neovascularization ability compare to control *in vivo* (Figure 17 and 18). Recently, several studies have suggested that the key elements for characterization of EPCs are the ability to form

vascular structures in proangiogenic surfaces *in vitro* and the capacity to contribute to the postnatal neovascularization process *in vivo* [38, 77-80]. According to this definition, the cells presented here correspond to EPCs. In addition, it is noteworthy that our cells share some similarities to late outgrowth endothelial cells (OECs) and endothelial colony forming cells (ECFCs). All these 3 groups of cells (OECs, ECFCs and VR-EPCs) exhibit cobblestone-like morphology, own highly proliferative potential and form capillary-like structures on matrigel [38, 80, 81]. Indeed, here we have found that VR-EPCs form capillary-like structures even on uncoated polystyrene surface (Figure 19A). Traditionally, EPCs can only form tube like structures on matrigel coated surface [82]. This new feature of the VR-EPCs may indicate an increased potential to develop micro-vessels compared to previously described EPCs.

Although here we show that endothelial environments increase both capillary –like structure formation and migration, yet the metabolic activity of the cells was significantly decreased when cultured in endothelial environment (Figure 19C). This finding is in agreement with previous reports, showing that under differentiation conditions, proliferation was suppressed [83] [84]. We also found nestin positive stem cells among the VR-EPCs. Although nestin is originally recognized as neural stem cell marker, several recent studies have shown the existence of nestin positive stem cells in rat cardiac tissue [85-87]. Furthermore, nestin positive stem cells have been described as a population that could contributes to the *de novo* vessel formation during myocardial infarction [87].

Although VR-EPCs might differentiate into different lineages *in vivo* since they have showed multilineage differentiation markers (Figure 22), cells only responded to endothelial environment *in vitro* and we did not observe any side effects after the administration of our cells *in vivo*. This might be due to the fact that VR-EPCs preferentially differentiate into endothelial cells. However, further studies have to be performed to evaluate the differentiation potential of VR-EPCs *in vivo*. In addition to the possibility of direct contributions to the vessel formation, paracrine effect is also another possible explanation for the increase in vascularization observed *in vivo*. Stem/ progenitor cells could induce vascularization also by secreting pre-angiogenic factors. It was demonstrated that EPCs released several pro-angiogenic factors which supported the ischemic tissue regeneration [70]. Bone marrow mononuclear cells improved cardiac function via both paracrine effects and direct differentiation [88]. In our study, we observed that VR-EPCs released cytokines related to angiogenesis and cytotaxis during *in vitro* culture (Figure 20), VEGF and PDGF which are growth factors strongly related to angiogenesis are of special relevance. Previous studies have shown that hypoxia and PDGF increased VEGF expression in several cell types [89]. Since dermal scaffolds provide a hypoxic environment *in vitro* and *in vivo*, increased levels of angiogenic factors are expected to be released during the dermal regeneration process *in vivo*. The chemokines secreted by our cells (CXCL-1 and MCP-1) may be a possible mechanism for the better *in vivo* cellularization (Figure 18B). However, the proliferation of our seeded cells inside the scaffold (Figure 15) may also contribute to this. Additionally, MCP-1 which is a chemokine mainly involved in tissue injury and inflammation can

directly induce angiogenesis via MCP-1-induced protein (MCPIP) [90] and also involved in arteriogenesis, which is a key process during tissue neovascularization [91].

From the first two sub-projects, we found that cells (stem/progenitor) releasing pro-angiogenic factors are possible candidate for neovascularization studies. Thus, we investigated whether genetic modified non-stem/progenitor cells releasing pro-angiogenic factors can be an alternative source for therapeutic neovascularization.

Although several technologies of gene therapy have been extensively applied in animal models of ischemia, their use in clinical settings is still limited [92]. Among the main reasons behind the poor clinical translation of animal studies of gene therapy into humans is the lack of a highly efficient gene delivery system and relatively easy procedures for the clinical translation. Here, we described a modified nucleofection technology based on alternative reagents which owns a high transfection efficiency (>80%) and also a relatively easy operation procedures. This technology might be a new therapeutic approach in the future.

Nucleofection technology is a newly developed nonviral transfection method based on electroporation technology. It could be useful for applications in gene therapy with autologous cells [93-95]. Many different approaches have been used for nucleofection based gene transfer into primary culture cells [96, 97]. Several previous studies have demonstrated the possibility to use this

technology to promote neovascularization in ischemic tissues. Aluigi et al have reported that nucleofection of human mesenchymal stem cells *in vitro* could produce gene expression for more than 20 days [93]. Although stem/progenitor cells were considered to be better candidates for *ex vivo* transfection, uncontrolled differentiation that could lead to a serious side effect was always a concern. Thus, in our study, the physiological stable autologous fibroblasts were used to deliver targeted genes into the ischemic tissue to demonstrate the efficiency of gene therapy. Compared with a recent study by Mueller *et al*, who demonstrated that a high-efficiency *ex vivo* rat dermal fibroblast transfection with VEGF nucleofection technology could induce local neovascularization effects in a rat skin flap model [98], our findings at least overcame two major drawbacks, namely the relative high cost and the low transfection efficiency (550 pg/ml peak expression of VEGF in the previous study [98] and 10ng/ml peak expression of VEGF in our present study). Our method cost only about 1 Euro per 1 million cells while the original method cost 12 Euro per 1 million cells. Thus, improved reagents for nucleofection in the present study will largely reduce the cost for high efficiency of nucleofection. This modified nucleofection may direct toward the development of similar protocols for human autologous cell gene therapy. However, it should be noted that much work may be needed to translate the findings from the present study to a clinical setting. Most importantly, there is a need to establish efficient protocols for preparation of primary cell cultures from human tissues and to establish the nucleofection efficiency of related genes into such cell cultures. In addition, the applicability for different ischemic diseases in human needs more careful evaluation because the ischemic changes or stages observed in the

animal model we used in the present study may be not necessarily seen under human conditions. Further studies using nucleofected primary cultures derived from human tissues are imperative for possible extension of our findings to a clinical trial.

The delivery of our cells directly into the middle part of the thigh is also another important aspect which may favor the therapeutic effects while lower the possible systematic side effects. Our results also confirmed a possible localized expression pattern. It was found that the plasmid can be detected for more than 28 days in the injected area, but it was undetectable in other organs after 14 days. The peak of expression of the plasmid *in vivo* was determined to occur on day 3 (Figure 24A), which is consistent with the *in vitro* data (Figure 23B). Although most of the previous studies showed that less than 10% of the plasmid can reach the general circulation after direct plasmid intramuscular injection [99, 100], it was reported that plasmid can be detected by PCR up to 1 year in mice [101]. Here, we showed that the use of *ex vivo* transfection has substantially decreased this time. When compared with the local plasmid concentration, the plasmids in the other organs were fairly low. On day 7, plasmid accumulation in the spleen could be explained by “cleaning effects” of the circulating plasmid by the immune system. All these findings indicate that autologous cell gene delivery can make sustained gene expression in the injected area locally.

After injections of gene-modified fibroblasts into an ischemia model, we also analyzed the neovascularization effects using a 3D micro-CT system. This

technology was used here because it has several advantages when compared with the planar area measurement methods. In our previous studies, angiographies had to be taken from different angles to obtain sufficient information about the collateral vessels [65, 68]. Even under the best circumstances, reliable collateral vessel counting is difficult to perform. In the present study, we were able to easily reconstruct the 3D structures of the ligated hindlimbs and quantify the collateral vessels in 3D views (Figure 25A and 25B). With the use of this method, we were also able to quantify the blood volume by voxel rendering in the reconstruction sections. Vessels related to arteriogenesis and angiogenesis were analyzed separately (Figure 27), and both were found to be improved after cell administration. This result was confirmed by measuring the blood flow in lower hindlimb (Figure 28). Using this technique, we analyzed the efficiency of this autologous cell therapy with gene delivery in the hindlimb ischemia model. Our results strongly suggest that autologous cell therapy with mixture of VEGF165 and bFGF nucleofected cells is very efficient to promote the formation and growth of collateral vessels and re-establish circulation in ischemic area of hindlimb.

In summary, in our studies for objective 3, we established a highly efficient modified nucleofection approach based gene delivery method using double transplantation of nucleofected primary fibroblasts. This technology owns two major advantages over other local application: 1) No exogenous vectors are needed; 2) High transfection efficiency with a relatively low cost. This technology might have the potential to be used in the future clinically.

7. GENERAL CONCLUSIONS AND PERSPECTIVES

This work supports the idea of using cell therapy for the induction of therapeutic vascularization. It is shown here that stem/progenitor or genetically modified cells can be used to increase vascularization in models of tissue regeneration or ischemia.

This thesis shows that stem cells derived from sweat glands or endothelial progenitor cells derived from cardiac tissue can be used for bio-activating dermal scaffolds *in vitro*, thus enhancing vascularization *in vivo*. Moreover, we also provide evidence suggesting that such increase could be triggered by vasculogenesis (direct cell differentiation) and/or by angiogenesis (paracrine factors). Although results are promising, several issues have to be addressed before clinical translation is possible. Among others the safety use of stem /progenitor cells have to be proven in long term *in vivo* experiments performed in large animal models. In addition, the regenerative potential of the two newly described cell populations have to be compared with other cells such as mesenchymal stem cells, which have been broadly described for their use in preclinical and clinical models of tissue regeneration and ischemia. Finally, in order to guarantee the feasibility of a new cell-based therapy, several legal obstacles will have to be taking in consideration.

In order to overcome the stem/progenitor cell obstacles, we also tried to induce neovascularization regardless of cell differentiation, here we have proved that gene modified cells secreting the angiogenic factors VEGF and bFGF could improve blood perfusion in hindlimb ischemia. Because all the protocols were

performed in order to be easily adapted for GMP protocol, this approach represents a step further for clinical translation.

8. REFERENCES

[1] Surgeons ASoP. Evidence-based clinical practice guideline: chronic wounds of the lower extremity. www.plasticsurgery.org 2007.

[2] Bjarnsholt T, Kirketerp-Moller K, Jensen PO, Madsen KG, Phipps R, Krogfelt K, Hoiby N, Givskov M. Why chronic wounds will not heal: a novel hypothesis. Wound Repair Regen 2008;16:2.

[3] Hafner J, Schaad I, Schneider E, Seifert B, Burg G, Cassina PC. Leg ulcers in peripheral arterial disease (arterial leg ulcers): impaired wound healing above the threshold of chronic critical limb ischemia. J Am Acad Dermatol 2000;43:1001.

[4] Clark RA, Ghosh K, Tonnesen MG. Tissue engineering for cutaneous wounds. J Invest Dermatol 2007;127:1018.

[5] Saltmarche AE. Low level laser therapy for healing acute and chronic wounds - the extendicare experience. Int Wound J 2008;5:351.

[6] Katarina H, Magnus L, Per K, Jan A. Diabetic persons with foot ulcers and their perceptions of hyperbaric oxygen chamber therapy. J Clin Nurs 2009;18:1975.

[7] Herscovici D, Jr., Sanders RW, Scaduto JM, Infante A, DiPasquale T. Vacuum-assisted wound closure (VAC therapy) for the management of patients with high-energy soft tissue injuries. J Orthop Trauma 2003;17:683.

[8] Ermolaeva SA, Varfolomeev AF, Chernukha MY, Yurov DS, Vasiliev MM, Kaminskaya AA, Moisenovich MM, Romanova JM, Murashev AN, Selezneva, II, Shimizu T, Sysolyatina EV, Shaginyan IA, Petrov OF, Mayevsky EI, Fortov VE, Morfill GE, Naroditsky BS, Gintsburg AL. Bactericidal effects of non-thermal argon plasma in vitro, in biofilms and in the animal model of

infected wounds. J Med Microbiol 2011;60:75.

[9] Mogford JE, Tawil B, Jia S, Mustoe TA. Fibrin sealant combined with fibroblasts and platelet-derived growth factor enhance wound healing in excisional wounds. Wound Repair Regen 2009;17:405.

[10] Falanga V, Iwamoto S, Chartier M, Yufit T, Butmarc J, Kouttab N, Shrayer D, Carson P. Autologous bone marrow-derived cultured mesenchymal stem cells delivered in a fibrin spray accelerate healing in murine and human cutaneous wounds. Tissue Eng 2007;13:1299.

[11] Nakao K, Morii N, Itoh H, Yamada T, Shiono S, Sugawara A, Saito Y, Mukoyama M, Arai H, Sakamoto M, et al. Atrial natriuretic polypeptide in brain--implication of central cardiovascular control. Klin Wochenschr 1987;65 Suppl 8:103.

[12] Turksen K, Rao M. Issues in human embryonic stem cell biology. Stem Cell Rev 2005;1:79.

[13] Carpenter MK, Couture LA. Regulatory considerations for the development of autologous induced pluripotent stem cell therapies. Regen Med;5:569.

[14] Zengin E, Chalajour F, Gehling UM, Ito WD, Treede H, Lauke H, Weil J, Reichenspurner H, Kilic N, Ergun S. Vascular wall resident progenitor cells: a source for postnatal vasculogenesis. Development 2006;133:1543.

[15] Petschnik AE, Klatte JE, Evers LH, Kruse C, Paus R, Danner S. Phenotypic indications that human sweat glands are a rich source of nestin-positive stem cell populations. Br J Dermatol;162:380.

[16] Asahara T, Murohara T, Sullivan A, Silver M, van der Zee R, Li T, Witzenbichler B, Schatteman G, Isner JM. Isolation of putative progenitor endothelial cells for angiogenesis. Science 1997;275:964.

[17] Asahara T, Kawamoto A. Endothelial progenitor cells for postnatal vasculogenesis. Am J Physiol Cell Physiol 2004;287:C572.

[18] Wang Y, Wan C, Deng L, Liu X, Cao X, Gilbert SR, Bouxsein ML, Faugere MC, Guldberg RE, Gerstenfeld LC, Haase VH, Johnson RS, Schipani E, Clemens TL. The hypoxia-inducible factor alpha pathway couples angiogenesis to osteogenesis during skeletal development. J Clin Invest 2007;117:1616.

[19] Scholz D, Cai WJ, Schaper W. Arteriogenesis, a new concept of vascular adaptation in occlusive disease. Angiogenesis 2001;4:247.

[20] Limbourg A, Korff T, Napp LC, Schaper W, Drexler H, Limbourg FP. Evaluation of postnatal arteriogenesis and angiogenesis in a mouse model of hind-limb ischemia. Nat Protoc 2009;4:1737.

[21] Matsunaga T, Warltier DC, Weihrauch DW, Moniz M, Tessmer J, Chilian WM. Ischemia-induced coronary collateral growth is dependent on vascular endothelial growth factor and nitric oxide. Circulation 2000;102:3098.

[22] Ravichandran R, Venugopal JR, Sundarrajan S, Mukherjee S, Ramakrishna S. Precipitation of nanohydroxyapatite on PLLA/PBLG/Collagen nanofibrous structures for the differentiation of adipose derived stem cells to osteogenic lineage. Biomaterials 2012;33(3):846.

[23] Zimmet H, Porapakkham P, Sata Y, Haas SJ, Itescu S, Forbes A, Krum H. Short- and long-term outcomes of intracoronary and endogenously mobilized bone marrow stem cells in the treatment of ST-segment elevation myocardial infarction: a meta-analysis of randomized control trials. Eur J Heart Fail. 2011 [Epub ahead of print]

[24] Le Bot N. Mammary gland stem cells. Nat Cell Biol;13:1294.

[25] Li L, Fukunaga-Kalabis M, Herlyn M. Isolation and Cultivation of Dermal Stem Cells that Differentiate into Functional Epidermal Melanocytes. Methods Mol Biol;806:15.

[26] Burba I, Colombo GI, Staszewsky LI, De Simone M, Devanna P, Nanni S, Avitabile D, Molla F, Cosentino S, Russo I, De Angelis N, Soldo A, Biondi A, Gambini E, Gaetano C, Farsetti A, Pompilio G, Latini R, Capogrossi MC, Pesce M. Histone deacetylase inhibition enhances self renewal and cardioprotection by human cord blood-derived CD34 cells. PLoS One;6:e22158.

[27] Kang Y, Park C, Kim D, Seong CM, Kwon K, Choi C. Unsorted human adipose tissue-derived stem cells promote angiogenesis and myogenesis in murine ischemic hindlimb model. Microvasc Res;80:310.

[28] Galli R, Borello U, Gritti A, Minasi MG, Bjornson C, Coletta M, Mora M, De Angelis MG, Fiocco R, Cossu G, Vescovi AL. Skeletal myogenic potential of human and mouse neural stem cells. Nat Neurosci 2000;3:986.

[29] Leroux L, Descamps B, Tojais NF, Seguy B, Oses P, Moreau C, Daret D, Ivanovic Z, Boiron JM, Lamaziere JM, Dufourcq P, Couffinhal T, Duplaa C. Hypoxia preconditioned mesenchymal stem cells improve vascular and skeletal muscle fiber regeneration after ischemia through a Wnt4-dependent pathway. Mol Ther;18:1545.

[30] Egana JT, Fierro FA, Kruger S, Bornhauser M, Huss R, Lavandero S, Machens HG. Use of human mesenchymal cells to improve vascularization in a mouse model for scaffold-based dermal regeneration. Tissue Eng Part A 2009;15:1191.

[31] Egana JT, Danner S, Kremer M, Rapoport DH, Lohmeyer JA, Dye JF, Hopfner U, Lavandero S, Kruse C, Machens HG. The use of glandular-derived

stem cells to improve vascularization in scaffold-mediated dermal regeneration. Biomaterials 2009;30:5918.

[32]Kruse C, Kajahn J, Petschnik AE, Maass A, Klink E, Rapoport DH, Wedel T. Adult pancreatic stem/progenitor cells spontaneously differentiate in vitro into multiple cell lineages and form teratoma-like structures. Ann Anat 2006;188:503.

[33]Dessapt-Baradez C, Reza M, Sivakumar G, Hernandez-Fuentes M, Markakis K, Gnudi L, Karalliedde J. Circulating vascular progenitor cells and central arterial stiffness in polycystic ovary syndrome. PLoS One;6:e20317.

[34]Terry T, Chen Z, Dixon RA, Vanderslice P, Zoldhelyi P, Willerson JT, Liu Q. CD34/M-cadherin bone marrow progenitor cells promote arteriogenesis in ischemic hindlimbs of ApoE/ mice. PLoS One;6:e20673.

[35]Kwon EJ, Lasiene J, Jacobson BE, Park IK, Horner PJ, Pun SH. Targeted nonviral delivery vehicles to neural progenitor cells in the mouse subventricular zone. Biomaterials;31:2417.

[36]Hristov M, Erl W, Weber PC. Endothelial progenitor cells: mobilization, differentiation, and homing. Arterioscler Thromb Vasc Biol 2003;23:1185.

[37]Quirici N, Soligo D, Caneva L, Servida F, Bossolasco P, Deliliers GL. Differentiation and expansion of endothelial cells from human bone marrow CD133(+) cells. Br J Haematol 2001;115:186.

[38]Yoder MC, Mead LE, Prater D, Krier TR, Mroueh KN, Li F, Krasich R, Temm CJ, Prchal JT, Ingram DA. Redefining endothelial progenitor cells via clonal analysis and hematopoietic stem/progenitor cell principals. Blood 2007;109:1801.

[39]Hur J, Yoon CH, Kim HS, Choi JH, Kang HJ, Hwang KK, Oh BH, Lee MM,

Park YB. Characterization of two types of endothelial progenitor cells and their different contributions to neovasculogenesis. Arterioscler Thromb Vasc Biol 2004;24:288.

[40] Ingram DA, Mead LE, Tanaka H, Meade V, Fenoglio A, Mortell K, Pollok K, Ferkowicz MJ, Gilley D, Yoder MC. Identification of a novel hierarchy of endothelial progenitor cells using human peripheral and umbilical cord blood. blood 2004;104:2752.

[41] Alessandri G, Girelli M, Taccagni G, Colombo A, Nicosia R, Caruso A, Baronio M, Pagano S, Cova L, Parati E. Human vasculogenesis ex vivo: embryonal aorta as a tool for isolation of endothelial cell progenitors. Lab Invest 2001;81:875.

[42] Nor JE, Christensen J, Mooney DJ, Polverini PJ. Vascular endothelial growth factor (VEGF)-mediated angiogenesis is associated with enhanced endothelial cell survival and induction of Bcl-2 expression. Am J Pathol 1999;154:375.

[43] Li B, Sharpe EE, Maupin AB, Teleron AA, Pyle AL, Carmeliet P, Young PP. VEGF and PlGF promote adult vasculogenesis by enhancing EPC recruitment and vessel formation at the site of tumor neovascularization. FASEB J 2006;20:1495.

[44] Asahara T, Bauters C, Zheng LP, Takeshita S, Bunting S, Ferrara N, Symes JF, Isner JM. Synergistic effect of vascular endothelial growth factor and basic fibroblast growth factor on angiogenesis in vivo. Circulation 1995;92:II365.

[45] Coppe JP, Kauser K, Campisi J, Beausejour CM. Secretion of vascular endothelial growth factor by primary human fibroblasts at senescence. J Biol

Chem 2006;281:29568.

[46] Ollivier V, Chabbat J, Herbert JM, Hakim J, de Prost D. Vascular endothelial growth factor production by fibroblasts in response to factor VIIa binding to tissue factor involves thrombin and factor Xa. Arterioscler Thromb Vasc Biol 2000;20:1374.

[47] Zhang Z, Ito WD, Hopfner U, Bohmert B, Kremer M, Reckhenrich AK, Harder Y, Lund N, Kruse C, Machens HG, Egana JT. The role of single cell derived vascular resident endothelial progenitor cells in the enhancement of vascularization in scaffold-based skin regeneration. Biomaterials;32:4109.

[48] Osella-Abate S, Quaglino P, Savoia P, Leporati C, Comessatti A, Bernengo MG. VEGF-165 serum levels and tyrosinase expression in melanoma patients: correlation with the clinical course. Melanoma Res 2002;12:325.

[49] Ostendorf T, Kunter U, Eitner F, Loos A, Regele H, Kerjaschki D, Henninger DD, Janjic N, Floege J. VEGF(165) mediates glomerular endothelial repair. J Clin Invest 1999;104:913.

[50] Shing Y, Folkman J, Haudenschild C, Lund D, Crum R, Klagsbrun M. Angiogenesis is stimulated by a tumor-derived endothelial cell growth factor. J Cell Biochem 1985;29:275.

[51] Tsuboi R, Rifkin DB. Recombinant basic fibroblast growth factor stimulates wound healing in healing-impaired db/db mice. J Exp Med 1990;172:245.

[52] Hayward P, Hokanson J, Heggers J, Fiddes J, Klingbeil C, Goeger M, Robson M. Fibroblast growth factor reserves the bacterial retardation of wound contraction. Am J Surg 1992;163:288.

[53] Fu X, Shen Z, Chen Y, Xie J, Guo Z, Zhang M, Sheng Z. Recombinant bovine basic fibroblast growth factor accelerates wound healing in patients

with burns, donor sites and chronic dermal ulcers. Chin Med J (Engl) 2000;113:367.

[54] Uchi H, Igarashi A, Urabe K, Koga T, Nakayama J, Kawamori R, Tamaki K, Hirakata H, Ohura T, Furue M. Clinical efficacy of basic fibroblast growth factor (bFGF) for diabetic ulcer. Eur J Dermatol 2009;19:461.

[55] Matziolis D, Tuischer J, Matziolis G, Kasper G, Duda G, Perka C. Osteogenic predifferentiation of human bone marrow-derived stem cells by short-term mechanical stimulation. Open Orthop J 2011;5:1.

[56] Lee MJ, Kim J, Lee KI, Shin JM, Chae JI, Chung HM. Enhancement of wound healing by secretory factors of endothelial precursor cells derived from human embryonic stem cells. Cytotherapy 2011;13:165.

[57] Hoch RV, Soriano P. Roles of PDGF in animal development. Development 2003;130:4769.

[58] Lohmeyer JA, Essmann E, Richerson SJ, Hagel C, Egana JT, Condurache A, Ganske P, Schulz K, Mailander P, Machens HG. Use of Erythropoietin as adjuvant therapy in nerve reconstruction. Langenbecks Arch Surg 2008;393:317.

[59] Anagnostou A, Liu Z, Steiner M, Chin K, Lee ES, Kessimian N, Noguchi CT. Erythropoietin receptor mRNA expression in human endothelial cells. Proc Natl Acad Sci U S A 1994;91:3974.

[60] Heeschen C, Aicher A, Lehmann R, Fichtlscherer S, Vasa M, Urbich C, Mildner-Rihm C, Martin H, Zeiher AM, Dimmeler S. Erythropoietin is a potent physiologic stimulus for endothelial progenitor cell mobilization. blood 2003;102:1340.

[61] Linssen MC, Engels W, Lemmens PJ, Heijnen VV, Van Bilsen M, Reneman

RS, van der Vusse GJ. Production of arachidonic acid metabolites in adult rat cardiac myocytes, endothelial cells, and fibroblast-like cells. Am J Physiol 1993;264:H973.

[62] Derhaag JG, Duijvestijn AM, Emeis JJ, Engels W, van Breda Vriesman PJ. Production and characterization of spontaneous rat heart endothelial cell lines. Lab Invest 1996;74:437.

[63] Egana JT, Condurache A, Lohmeyer JA, Kremer M, Stockelhuber BM, Lavandero S, Machens HG. Ex vivo method to visualize and quantify vascular networks in native and tissue engineered skin. Langenbecks Arch Surg 2009;394:349.

[64] Geback T, Schulz MM, Koumoutsakos P, Detmar M. TScratch: a novel and simple software tool for automated analysis of monolayer wound healing assays. Biotechniques 2009;46:265.

[65] Herzog S, Sager H, Khmelevski E, Deylig A, Ito WD. Collateral arteries grow from preexisting anastomoses in the rat hindlimb. Am J Physiol Heart Circ Physiol 2002;283:H2012.

[66] Ito WD, Arras M, Scholz D, Winkler B, Htun P, Schaper W. Angiogenesis but not collateral growth is associated with ischemia after femoral artery occlusion. Am J Physiol 1997;273:H1255.

[67] S N. Gene therapy of cardiovascular disease. Curr Opin Mol Ther 2008;10:479.

[68] Khmelewski E, Becker A, Meinertz T, Ito WD. Tissue resident cells play a dominant role in arteriogenesis and concomitant macrophage accumulation. Circ Res 2004;95:E56.

[69] Tashiro K, Inamura M, Kawabata K, Sakurai F, Yamanishi K, Hayakawa T,

Mizuguchi H. Efficient adipocyte and osteoblast differentiation from mouse induced pluripotent stem cells by adenoviral transduction. Stem Cells 2009;27:1802.

[70] Urbich C, Aicher A, Heeschen C, Dernbach E, Hofmann WK, Zeiher AM, Dimmeler S. Soluble factors released by endothelial progenitor cells promote migration of endothelial cells and cardiac resident progenitor cells. J Mol Cell Cardiol 2005;39:733.

[71] Ojeh NO, Frame JD, Navsaria HA. In vitro characterization of an artificial dermal scaffold. Tissue Eng 2001;7:457.

[72] Sun L, Akiyama K, Zhang H, Yamaza T, Hou Y, Zhao S, Xu T, Le A, Shi S. Mesenchymal stem cell transplantation reverses multiorgan dysfunction in systemic lupus erythematosus mice and humans. Stem Cells 2009;27:1421.

[73] Liang J, Zhang H, Hua B, Wang H, Lu L, Shi S, Hou Y, Zeng X, Gilkeson GS, Sun L. Allogenic mesenchymal stem cells transplantation in refractory systemic lupus erythematosus: a pilot clinical study. Ann Rheum Dis;69:1423.

[74] Caplan AI, Dennis JE. Mesenchymal stem cells as trophic mediators. J Cell Biochem 2006;98:1076.

[75] Distler JH, Hirth A, Kurowska-Stolarska M, Gay RE, Gay S, Distler O. Angiogenic and angiostatic factors in the molecular control of angiogenesis. Q J Nucl Med 2003;47:149.

[76] Yang C, Zhu P, Yan L, Chen L, Meng R, Lao G. Dynamic changes in matrix metalloproteinase 9 and tissue inhibitor of metalloproteinase 1 levels during wound healing in diabetic rats. J Am Podiatr Med Assoc 2009;99:489.

[77] Timmermans F, Plum J, Yoder MC, Ingram DA, Vandekerckhove B, Case J. Endothelial progenitor cells: identity defined? J Cell Mol Med 2009;13:87.

[78] Yao H, Liu B, Wang X, Lan Y, Hou N, Yang X, Mao N. Identification of high proliferative potential precursors with hemangioblastic activity in the mouse aorta-gonad- mesonephros region. Stem Cells 2007;25:1423.

[79] Hirschi KK, Ingram DA, Yoder MC. Assessing identity, phenotype, and fate of endothelial progenitor cells. Arterioscler Thromb Vasc Biol 2008;28:1584.

[80] Watt SM, Athanassopoulos A, Harris AL, Tsaknakis G. Human endothelial stem/progenitor cells, angiogenic factors and vascular repair. J R Soc Interface 2011;7 Suppl 6:S731.

[81] Richardson MR, Yoder MC. Endothelial progenitor cells: Quo Vadis? J Mol Cell Cardiol 2011;50:266.

[82] Kleinman HK, Martin GR. Matrigel: basement membrane matrix with biological activity. Semin Cancer Biol 2005;15:378.

[83] Xia K, Xue H, Dong D, Zhu S, Wang J, Zhang Q, Hou L, Chen H, Tao R, Huang Z, Fu Z, Chen YG, Han JD. Identification of the proliferation/differentiation switch in the cellular network of multicellular organisms. PLoS Comput Biol 2006;2:e145.

[84] Brown G, Hughes PJ, Michell RH. Cell differentiation and proliferation--simultaneous but independent? Exp Cell Res 2003;291:282.

[85] Beguin PC, El-Helou V, Assimakopoulos J, Clement R, Gosselin H, Brugada R, Villeneuve L, Rohlicek CV, Del Duca D, Lapointe N, Rouleau JL, Calderone A. The phenotype and potential origin of nestin+ cardiac myocyte-like cells following infarction. J Appl Physiol 2009;107:1241.

[86] El-Helou V, Dupuis J, Proulx C, Drapeau J, Clement R, Gosselin H, Villeneuve L, Manganas L, Calderone A. Resident nestin+ neural-like cells and fibers are detected in normal and damaged rat myocardium. Hypertension

2005;46:1219.

[87] Hoffman RM. The potential of nestin-expressing hair follicle stem cells in regenerative medicine. Expert Opin Biol Ther 2007;7:289.

[88] Yoon CH, Koyanagi M, Iekushi K, Seeger F, Urbich C, Zeiher AM, Dimmeler S. Mechanism of improved cardiac function after bone marrow mononuclear cell therapy: role of cardiovascular lineage commitment. Circulation;121:2001.

[89] Petersen W, Pufe T, Zantop T, Tillmann B, Mentlein R. Hypoxia and PDGF have a synergistic effect that increases the expression of the angiogenetic peptide vascular endothelial growth factor in Achilles tendon fibroblasts. Arch Orthop Trauma Surg 2003;123:485.

[90] Niu J, Azfer A, Zhelyabovska O, Fatma S, Kolattukudy PE. Monocyte chemotactic protein (MCP)-1 promotes angiogenesis via a novel transcription factor, MCP-1-induced protein (MCPIP). J Biol Chem 2008;283:14542.

[91] Ito WD, Arras M, Winkler B, Scholz D, Schaper J, Schaper W. Monocyte chemotactic protein-1 increases collateral and peripheral conductance after femoral artery occlusion. Circ Res 1997;80:829.

[92] Choo PW, Rand CS, Inui TS, Lee ML, Ma CC, Platt R. A pharmacodynamic assessment of the impact of antihypertensive non-adherence on blood pressure control. Pharmacoepidemiol Drug Saf 2000;9:557.

[93] Aluigi M, Fogli M, Curti A, Isidori A, Gruppioni E, Chiodoni C, Colombo MP, Versura P, D'Errico-Grigioni A, Ferri E, Baccarani M, Lemoli RM. Nucleofection is an efficient nonviral transfection technique for human bone marrow-derived mesenchymal stem cells. Stem Cells 2006;24:454.

[94] Cesnulevicius K, Timmer M, Wesemann M, Thomas T, Barkhausen T, Grothe C. Nucleofection is the most efficient nonviral transfection method for neuronal stem cells derived from ventral mesencephali with no changes in cell composition or dopaminergic fate. Stem Cells 2006;24:2776.

[95] Jacobsen F, Mertens-Rill J, Beller J, Hirsch T, Daigeler A, Langer S, Lehnhardt M, Steinau HU, Steinstraesser L. Nucleofection: a new method for cutaneous gene transfer? J Biomed Biotechnol 2006;2006:26060.

[96] Zeitelhofer M, Vessey JP, Thomas S, Kiebler M, Dahm R. Transfection of cultured primary neurons via nucleofection. Curr Protoc Neurosci 2009;Chapter 4:Unit4 32.

[97] Kang J, Ramu S, Lee S, Aguilar B, Ganesan SK, Yoo J, Kalra VK, Koh CJ, Hong YK. Phosphate-buffered saline-based nucleofection of primary endothelial cells. Anal Biochem 2009;386:251.

[98] Mueller CK, Thorwarth MW, Schultze-Mosgau S. Angiogenic gene-modified fibroblasts for induction of localized angiogenesis. J Surg Res;160:340.

[99] Gravier R, Dory D, Laurentie M, Bougeard S, Cariolet R, Jestin A. In vivo tissue distribution and kinetics of a pseudorabies virus plasmid DNA vaccine after intramuscular injection in swine. Vaccine 2007;25:6930.

[100] Parker SE, Monteith D, Horton H, Hof R, Hernandez P, Vilalta A, Hartikka J, Hobart P, Bentley CE, Chang A, Hedstrom R, Rogers WO, Kumar S, Hoffman SL, Norman JA. Safety of a GM-CSF adjuvant-plasmid DNA malaria vaccine. Gene Ther 2001;8:1011.

[101] Bembenek A, Lotterer E, Machens A, Cario H, Krause U, Holzhausen HJ, Fleig WE, Dralle H. Neuroendocrine tumor of the common hepatic duct: a

rare cause of extrahepatic jaundice in adolescence. Surgery 1998;123:712.

APPENDIX

Published peer-reviewed papers by PhD candidate during study period

1) Zhang Z, Ito WD , Hopfner U, Böhmert B, Harder Y, Reckhenrich A, Kremer M, Lund N, Kruse C, Machens HG Egaña JT. The Role of Single Cell Derived Vascular Resident Endothelial Progenitor Cells in the Enhancement of Vascularization in Scaffold-based Skin Regeneration. *Biomaterials*. 2011 Jun;32(17):4109-17. Impact factor 2010: 7.8

2) Zhang Z, Slobodianski A, Ito WD, Arnold A, Nehlsen J, et al. (2011) Enhanced Collateral Growth by Double Transplantation of Gene-Nucleofected Fibroblasts in Ischemic Hindlimb of Rats. *PLoS ONE* 6(4): e19192. Impact factor 2010:4.4

3) Zhang Z, Egaña JT, Machens HG, A.F Schilling. Cell-based resorption assays for bone graft substitutes. *Acta Biomater.* 2012 Jan;8(1):13-9. Epub 2011 Sep 24. Impact factor 2010: 4.8

4) Reckhenrich AK, Hopfner U, Krötz F, **Zhang Z**, Koch C, Kremer M, Machens HG , Plank C, Egaña JT. Bioactivation of dermal scaffolds with a non-viral Copolymer-protected gene vector. *Biomaterials*; 2011 Mar; 32(7):1996-2003. Epub 2010 Dec 14. Impact factor 2010: 7.8

5) Danner S, Kremer M2, Petschnik AE, Nagel S, **Zhang Z**, Hopfner U, Reckhenrich AK, Weber C, Schenck TL, Becker T, Kruse C, Machens HG, Egaña JT. The Use of Human Sweat Gland-derived Stem Cells for Enhancing Vascularization during Dermal Regeneration. (Accepted by *Journal of Investigative Dermatology* Impact factor 2010: 6.2)

6) Das D, **Zhang Z**, Winkler T, Mour M, Günter CI, Morlock MM, Machens HG, Schilling AF. Bioresorption and Degradation of Biomaterials. *Adv Biochem Eng Biotechnol.* 2011 Oct 6. [Epub ahead of print] Impact factor 2010: 2.2